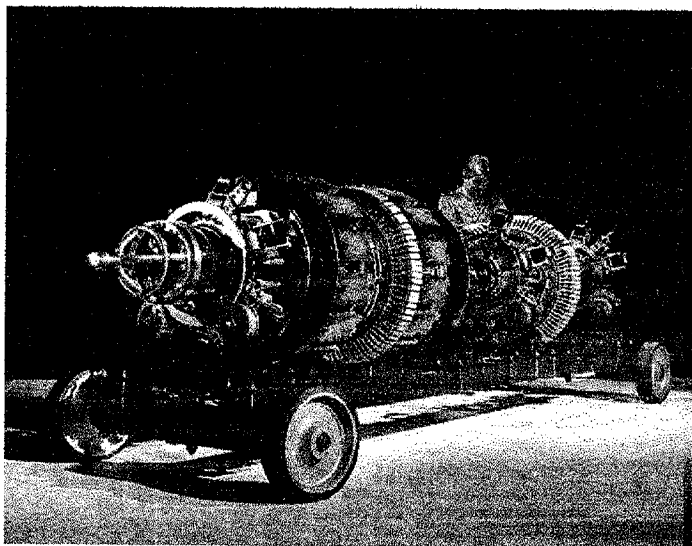


**PIPELINE INSPECTION, MAINTENANCE AND
PERFORMANCE INFORMATION SYSTEM
PROGRESS REPORT**



Spring 1998

**Botond Farkas
Prof. R.G. Bea**

**University of California at Berkeley
Marine Technology Group**

Table of Contents

Executive Summary	p. ii
Introduction.....	p. 1
Corrosion Rate	p. 3
Derivation of the Corrosion Loss Equation	p. 3
Calibration of the Corrosion Loss Equation	p. 5
Calibration of the Corrosion Loss Equation for Unpiggable Pipelines	p. 10
Biocorrosion	p. 10
Types of Bacteria Associated with Sulfate Reduction.....	p. 12
Effect of pH on P and N	p. 16
Effect of Flow Regime on the Value of P and N	p. 18
Burst Strength of a Corroded Pipe	p. 23
Reliability of Pipelines	p. 29
Example Application	p. 32
Conclusion	p. 34
References.....	p. 35
Appendix A.....	p. 39
Appendix B	p. 43

Executive Summary

An equation for the corrosion loss in a multiphase pipeline and in an oil pipeline has been developed, through the use of literary sources and analytical tools. The equation is based on the principles of the biocorrosion process. Biocorrosion in the United States has caused serious problems due to the souring of wells by sulfate reducing bacteria, which produce an environment that is hostile to ferrous compounds.

The calibration of the developed empirical equation was carried out with the aid of existing atmospheric corrosion data that was adjusted to the environment in a pipeline. The effects of flow were also incorporated into the final solution, and the effect of localized pH due to bacterial action was also accounted for.

A simplified equation for the burst pressure of a corroded pipe has also been developed. The equation is the result of an effort to match research results developed by Shell and ARCO Alaska Inc. The resulting equation deviates from the work performed by Shell and ARCO by 7% at most, to as little as a ½ %. All equations used for the research are restricted to be used for corrosion that is between 20% and 80% of the wall thickness. Outside this range the equations lose their validity.

Finally, the foregoing developments were combined to provide a reliability calculation for pipelines in the marine environment, and an example application of the processes is presented at the end of this report. Care should be taken however when applying the developed methods, due to the fact that extensive testing has not been done to provide a suitable confidence level in the developed method for calculating the reliability of pipelines.

Introduction

Corrosion of pipelines in the offshore oil industry has been a major problem for years, and many industry leaders have tried to tackle the problem from various angles. One way corrosion can be arrested is through the application of a barrier like paint or a plastic lining, that is able to separate the corroding surface from the corrosive environment, thus reducing the potential for corrosion. Corrosion inhibition can also be accomplished through the use of cathodic protection, through the use of corrosion resistant materials, or through the conditioning of the environment in which the corroding material is to be placed. Often, these solutions lose their effectiveness with time, and then the pipelines have to be inspected.

The major problem with the inspection of pipelines is that some are difficult to access, and therefore to obtain any useful information about the state of the pipeline, expensive diving operations are needed. Some pipelines can be accessed through the use of “intelligent pigs”, that are able to use magnetic flux leakage sensors to gather information about the state of the pipeline. Other pipelines are too small for the pigs, or they have such a geometry that pigs can't maneuver easily along the pipeline's length.

Therefore to save money, and to reduce the risk of accidents caused by the failure of corroded pipelines, it is important to be able to predict the extent of corrosion in any specific pipeline without having to inspect the pipeline manually. For pipelines that can be pigged, the task of determining the reliability of the system is straightforward, while the task of determining the reliability of an unpiggable pipeline runs into several obstacles.

This report will focus on obtaining the reliability of both piggable and unpiggable pipelines, as well as on obtaining the burst pressure of a corroded pipe. By knowing the capacity, the demand and the standard deviation of the capacity and the demand, the reliability of a pipeline system can be found. The key component for assessing the pipeline's reliability is to correctly determine the corrosion loss in the pipeline, and then calculate the capacity of the pipeline.

Throughout the course of the research a continuing effort will be made to correctly assess the corrosion problem of ferrous compounds in various environments. As additional information is obtained, the model will be updated periodically. By correctly determining the

corrosion rate in a pipeline, along with the allowable pressure that the pipeline can be operated at, accidents can be avoided, and pipelines can be kept in service longer through the application of preventive maintenance.

I. Corrosion Rate

Corrosion is a major problem for the engineering industry, and the potential for savings that corrosion control can provide is constantly on the rise. Industries are realizing that by controlling the corrosion problem through practicing preventive maintenance, more can be gained than by neglect of the problem.

The key to understanding the corrosion problem is to be able to accurately predict the nature of the reaction taking place at the interface of the corroding material and the environment. Careful experiments and meticulous records of the results of these experiments have to be made. An empirical process would result in the best solution to the corrosion problem, but the experiments would have to be case specific. Also, enough of these experiments have to be performed to build up a significant population, which could provide a reasonable confidence limit. This approach is both time and labor intensive, and costs money. Therefore the method used to derive a representative formula for the corrosion rate of ferrous compounds, was to fit a curve to existing data and then to calibrate the equation of the curve for various environments. As more and more data is gathered, the equation can be calibrated better and better.

A. Derivation of the Corrosion Loss Equation

According to various published sources, the corrosion loss with time in ferrous compounds takes the shape represented in Figure 1. This curve is similar to an n^{th} degree polynomial, and the equation of the curve can be derived through the process of curve fitting. The problem with a polynomial equation though is that it is case specific, unless the constants and the powers are left as variables. Also, the more degrees the polynomial has the more accurate it is, but this would result in more terms. When the variables are introduced into the problem, the task of how to choose the variables becomes the main concern. The selection of the variables will highly depend upon the environment where the metal is placed. This requires the individual applying the equation to know a lot about where the corrosion loss is to be evaluated, sometimes know more than is humanly possible.

Therefore the polynomial solution was rejected and a different approach was used. It can be seen in Figure 2 that a polynomial solution can be approximated by the combination of a

logarithmic function and a linear function. After some trial and error, Equation 1 was derived. This equation has a component that is logarithmic, along with a power function, which provide

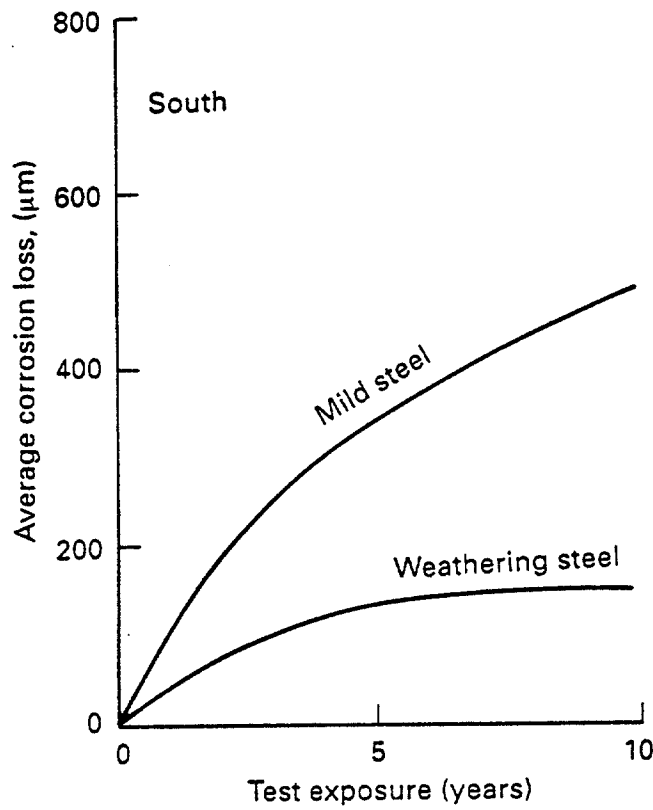


Figure 1: Typical corrosion loss curve. [8]

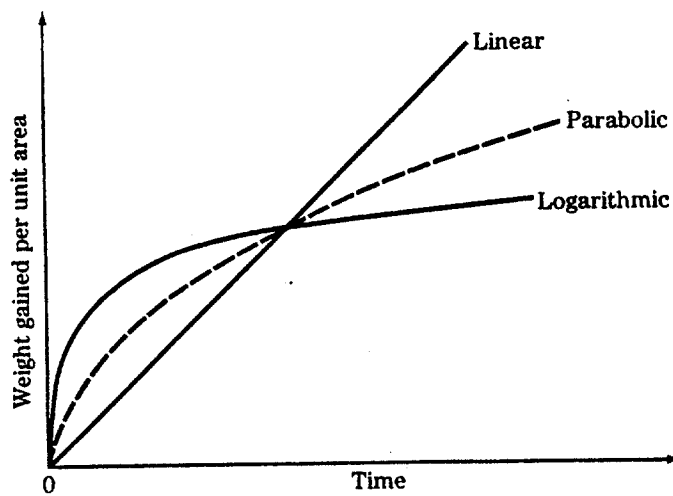


Figure 2: Oxidation rate laws. [9]

the general shape of the corrosion loss curve. The exponential term and the inverse t term in the equation only control the corrosion loss for the first couple of years and then the terms decay to a value of 1 with higher values of t.

$$CorrosionLoss = \left[1 + e^{(1-Nt)} \right] \left[\log(1+t)^P \right] \left[1 + \frac{1}{(1+t)} \right] \left[t^{\frac{1}{3}} \right] \quad \text{(Eq. 1)}$$

In Equation 1, the variables N and P serve as shaping parameters, and depend upon the type of environment where the corrosion loss is being calculated. The variable t in the equation is measured in years.

Once the general form of the corrosion loss is known, the equation has to be calibrated in order that it may be applied to any specific case. The goal of this research however was to obtain a bound on the corrosion problem in pipelines and risers, therefore the effort of calibrating the equation was focused around this area.

B. Calibration of the Corrosion Loss Equation

To calibrate the corrosion loss equation, several references [6, 8] were used to supply corrosion loss data. The collection of data from these sources has been tabulated and is included in Appendix A. Most of the data available is for a limited number of metals, therefore the effort of calibration was focused around the type of metals on which there is considerable information. These metals include iron, mild steel or carbon steel, low alloy steels, stainless steels, and nickel iron alloys.

One drawback of using the existing data is that not only is this data for atmospheric corrosion, but the numbers supplied are for various environments, various exposure times, and sometimes values of either corrosion loss or corrosion rate are given. For the corrosion loss data, Equation 1 was applied, and a fit of the curve for the value provided was accomplished through trial and error. Sometimes more than one value of P and N were able to fit the curve for the existing point, therefore all possible combinations of P and N were calculated and then averaged.

For the corrosion rate data, the same approach was used as with the corrosion loss, but first the equation for the corrosion rate was calculated. The corrosion rate equation is simply the derivative of the corrosion loss equation, and takes the following form:

$$CorrosionRate = \left[1 + e^{(1-N)} \right] \left[\log(1+t)^P \right] \left[1 + \frac{1}{(1+t)} \right] \left[t^{\frac{1}{3}} \right] \left\{ \frac{1}{3t} - \frac{1}{(1+t)^2 + (1+t)} + \frac{\log(e)}{[\log(1+t)](1+t)} - N \frac{e^{(1-N)}}{1 + e^{(1-N)}} \right\}$$

(Eq. 2)

Again, for various values of the corrosion rate corresponding to certain exposure times, the curve was calibrated to fit the data point available, and when all the possible combinations of P and N were obtained, the mean was calculated. The results for the various mean values of P and N are tabulated in Table 1.

*VALUES FOR ATMOSPHERIC CORROSION	IRON	MILD CARBON STEEL	LOW ALLOY STEELS	STAINLESS STEELS	NICKEL IRON ALLOYS
Mean "P"	7.48	15.03	9.38	0.47	16.90
Mean "N"	3.00	3.48	1.90	~	~
Coefficient of Variation of "P"	32%	103%	81%	67%	88%
Coefficient of Variation of "N"	94%	124%	75%	~	~

Table 1: Results of statistical analysis performed on fitting parameters P and N.

Due to the fact that only a limited population was available to obtain the results tabulated in Table 1, several adjustments to the values of P and N for the various metals was needed. With increasing values of P, the corrosion loss or rate increases, but it is well known that nickel iron alloys have a lower potential to corrode than mild steels, therefore the value of P for nickel iron alloys in Table 1 can't be correct. Very little data was available for all the metals except mild steels, therefore the value of P for mild steel was retained, while the values for the other metals were adjusted around this value.

Corrosion Rate

The value of N does not influence the corrosion rate or loss at large time values, therefore this parameter does not play an important part in the result of long term analysis. The value N however is important if only the short-term corrosion effects have to be calculated. In this case larger values of N tend to reduce the corrosion loss at the early stages of corrosion, while lower values of N result in a sharp rise in the corrosion loss. An illustration of how values of N influence corrosion loss can be seen in Figure 3.

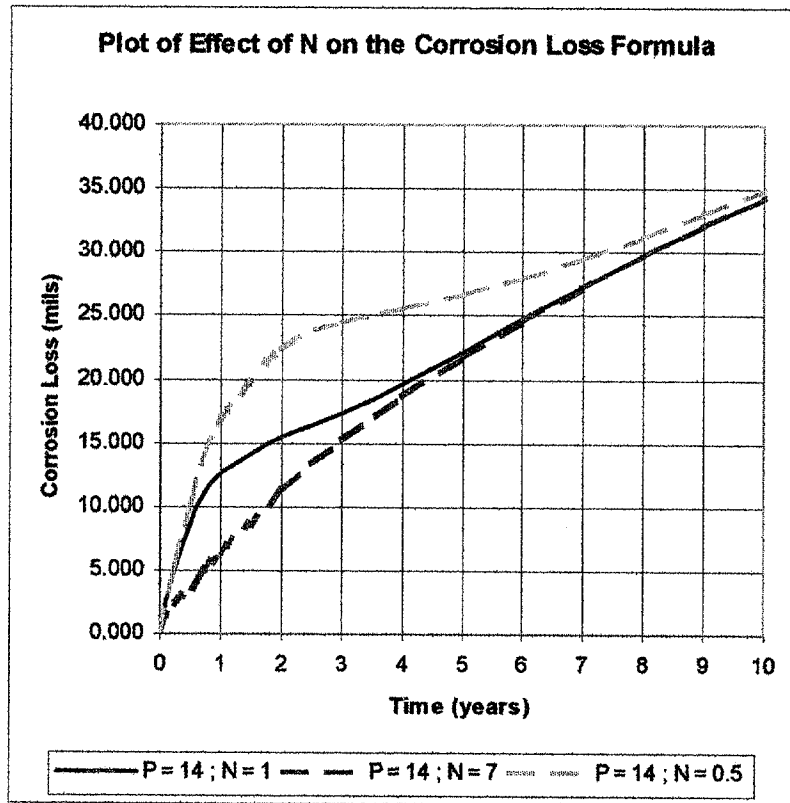


Figure 3: Effect of N on corrosion loss.

To finalize the standard values of P and N for various metals, intuitive judgement and general knowledge of the metals was used. These final values can be seen in Table 2, but it must be kept in mind that the representative values in the table are for corrosion in an atmospheric environment. In a pipeline however, localized pH values can drop as low as one, and in this case the values of P and N have to be adjusted accordingly.

*VALUES FOR ATMOSPHERIC CORROSION	P	N
Mild Steel	14	1.5
Low Alloy Steel	10	2
Nickel Iron Alloys	5	3.5
Stainless Steel	1.5	7
Titanium	0.25	10

Table2: Typical values of N and P for various materials

The graphical representation of corrosion loss for the values shown in Table 2 can be seen in Figure 4.

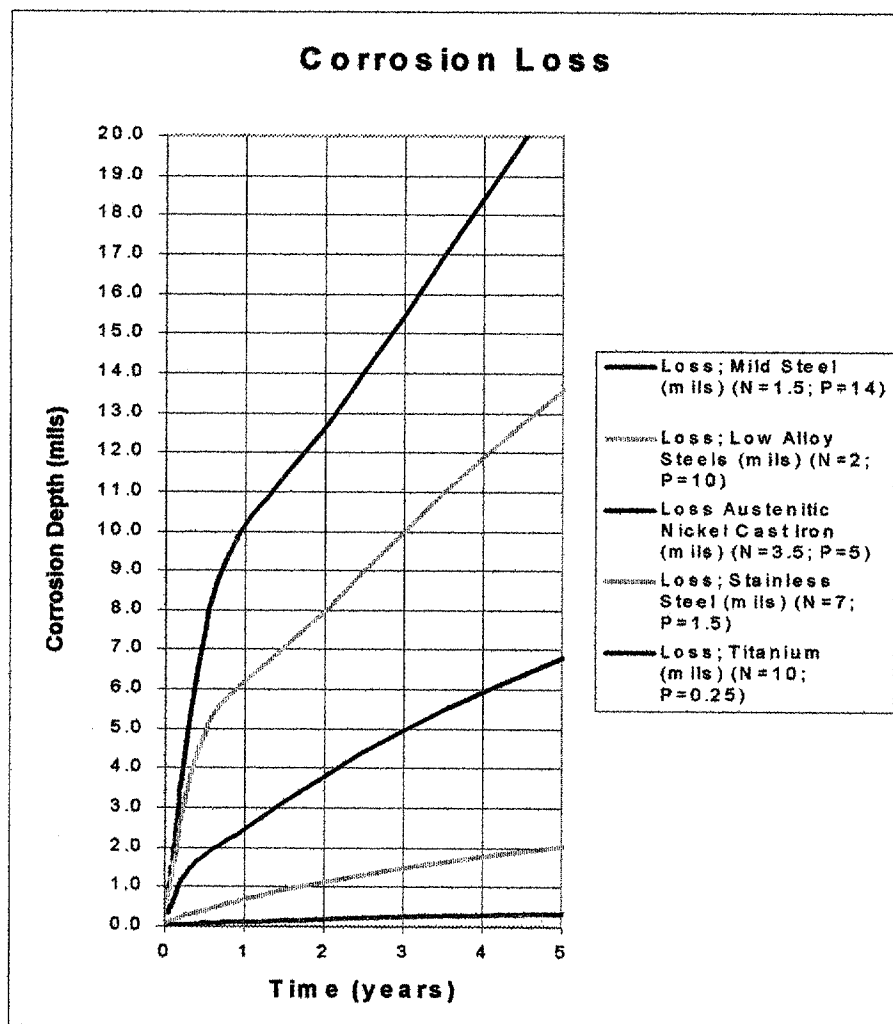


Figure 4: Theoretical corrosion loss experienced by various materials due to average atmospheric conditions.

The next step in calibrating the equation for corrosion loss is to analyze the specific environment where it is to be applied. Since there are many specific environments where the equation can be utilized, to keep the problem reasonably simple one such environment was chosen. The specific environment chosen was that in which oil and gas is transported over long distances, and where secondary recovery techniques like pumping water into the wells are utilized.

II. Calibration of the Corrosion Loss Equation for Unpiggable Pipelines

A. Biocorrosion

Before further calibration of the corrosion loss equation is possible, the major causes of corrosion in pipelines have to be examined. It has been stated earlier that corrosion is a problem in pipelines in the United States due to the fact that many of the wells are of a sour nature.

Souring of the wells can be largely attributed to microbial activity, where through the aid of bacteria, hydrogen sulfide is produced. Other sulfur compounds will also be present and all these compounds react with iron or steel when contact is made. When exposed to sulfur species, iron and steel first develop a weak protective film of mackinawite (an iron sulfide rich in iron) that later changes through different chemical and electrochemical paths to more stable iron sulfides. [7]

In all cases iron sulfides are characterized by their marked cathodic effects on the hydrogen reduction reaction, which leads to an increase in the corrosion rate. In many cases the biocorrosion process is related to the passivity breakdown by metabolic products having aggressive characteristics which are introduced into the medium by the activity of sulfate reducing bacteria (SRB). Also, other anions able to facilitate localized corrosion are frequently present in the environment, such as the widely distributed chlorides that enhance the aggressiveness of sulfur compounds. [7]

The biocorrosion attack can be attributed to the capacity of the bacteria to uptake hydrogen by the means of their enzymatic systems (hydrogenase), which in turn produces ferrous sulfide and ferrous hydroxide, corrosion byproducts. The three elements of biocorrosion are illustrated in Figure 5.

It has been noticed however by certain researchers that the settlement of a bacterial film on a carbon steel surface previously coated with an iron sulfide film can diminish the spalling of this film, but cannot avoid the localized corrosion hazard. Usually corrosion affects areas where there are defects in the iron sulfide film or metal matrix. Hence, the role of environmental conditions are very important in determining the chemical structure and physical form of the iron sulfides that, in turn, condition the rate and extent of the corrosion. [7]

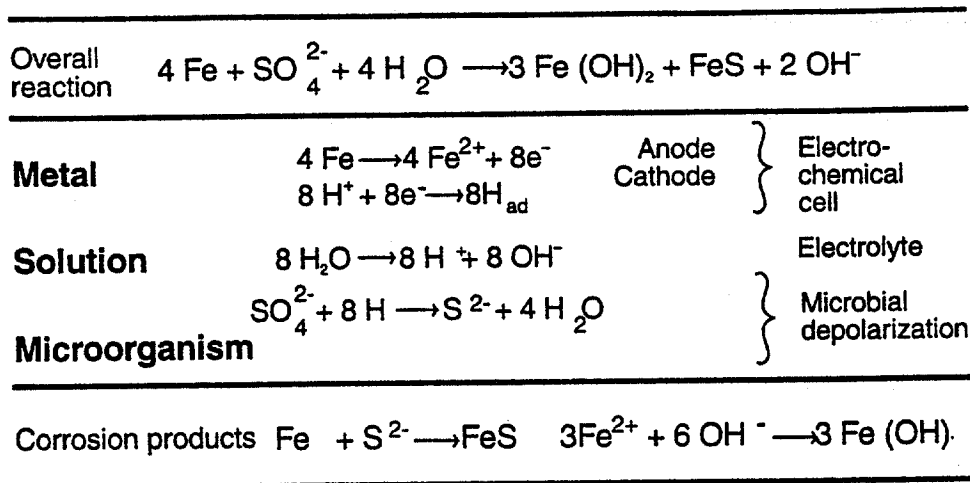


Figure 5: The three elements of biocorrosion.[7]

The rate of corrosion is also affected by the presence of oxygen, therefore the less oxygen present in the system the better are the chances of the metal not corroding. As a biofilm attaches to the surface of the metal, with time it grows and after a certain time period it becomes thick enough to prevent the efficient diffusion of oxygen to the metal-biofilm interface. When this occurs, at the bottom of the biofilm there are strictly anaerobic bacteria. The bacterial deposits therefore create a differential availability of oxygen at the metal surface. Note however, that sulfate can also act as a terminal electron acceptor, instead of oxygen, so eliminating oxygen from the system might not necessarily stop the corrosion process. [7] A differential aeration cell can be seen in Figure 6.

In Figure 6 the area with the lowest oxygen availability (under the deposit) is forced to become the anode in the reaction, while the area outside the deposit acts as the cathode (in this case through the microbial mucilage). The explanation of the previous statement is the following. On a microscopic scale, a metal is rarely uniform and each grain will have slightly different surface characteristics and oxygen availability from its neighbors. At any time, some of the grains will be acting as anodes while others will be acting as cathodes. A fraction of a second later, the conditions may be reversed, and these constantly changing anodic and cathodic sites

explain why a metal shows uniform rusting over its entire surface. In the case of biocorrosion however, the area under the biofilm has no access to oxygen, therefore it becomes the anode. [7]

It is evident therefore that sulfate reducing bacteria act on corrosion in an indirect way, due to their ability to produce hydrogen sulfide that could be used as a cathodic reactant (removes electrons from metal). This in turn determines whether an area on a metal surface will be anodic or cathodic.¹ [7]

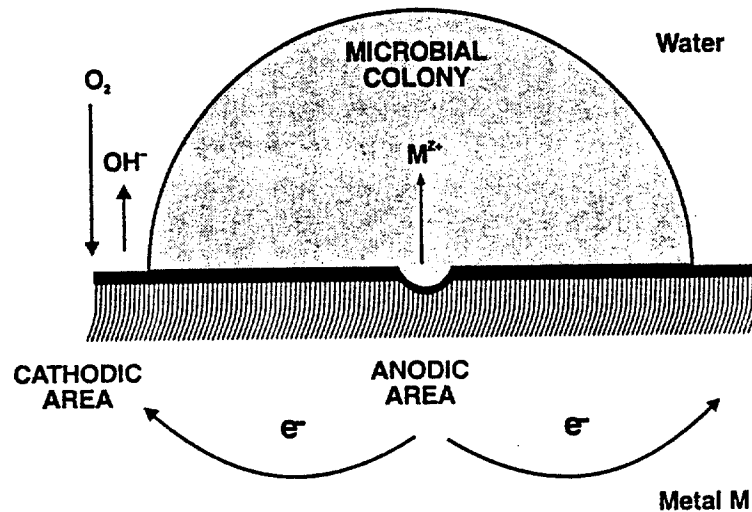


Figure 6: Simplified scheme of biocorrosion beneath a bacterial colony.[7]

B. Types of Bacteria Associated with Sulfate Reduction

Sulfate reducing bacteria (SRB) are prokaryotic microorganisms, which means that they lack a definite nucleus, and reproduce through binary fission. These bacteria are also heterotrophes, therefore an external source of carbon is required for their growth. Some recent studies have suggested that there is a wide range of carbon sources that these bacteria can use for their growth. Several species are able to use acetate as the sole carbon source, and in the case of marine SRB, the limiting factor for growth is not the sulfate ion but the concentration of the carbon source available in the seawater.

¹ **Cathode:** site on metal surface where electrons are removed
Anode: site on metal surface where metal ions go into solution

A list of sulfate reducing bacteria and their characteristics can be found in Table 3.

Table 3

Prokaryotic Microorganisms

Thiobacillus	Aerobic; use carbon dioxide as their main carbon source; rate of sulfur oxidation depends on the type of sulfur compound used; Need an average sodium chloride concentration of ca. 0.5 M. Frequently its aggressiveness is enhanced through the formation of microbial consortia with anaerobic SRB, or in certain environments called "sulphuretum" in which part or whole of the sulfur cycle takes place.
Thiobacillus Denitrificans	able to grow anaerobically by using nitrates as the final electron acceptor
Thiobacillus Thiooxidans	Ability to oxidize 31 g of sulfur per gram of carbon; pH on the order of 0.50 Able to produce an important amount of sulfur or decrease the environmental pH to 0.50
Thiobacillus Thioparus	Sulfur oxidizing bacteria, generally short, thick rods ranging from 0.5 to 3.0 μm ; Being aerobic and autotrophic, they are able to synthesize complex organic compounds They do not use organic compounds as nutrients; Optimal temperature for growth is 25 - 30 deg Celsius; Oxidizes thiosulfate to sulfate and sulfur; This species also oxidizes elemental sulfur to sulfate, although it is not able to oxidize sulfide. Oxidation reactions begin at pH ~ 7.8, and after completing their growth they can reach values of 4.5
Thiobacillus Concretivorus	Oxidizes thiosulfate using tetrathionate as an intermediate reaction compound and also oxidizes elemental sulfur and sulfide. The optimal pH range for growth is 1 - 4.
Thiobacillus Ferrooxidans	generally related to the iron oxidizing bacteria through its ability to oxidize inorganic ferrous compounds; It also obtains energy from thioulfate oxidation. Its natural habitats are acidic waters with high iron content, and much of the literature on this bacterium is related to the bioleaching process. It is an obligate autotroph that grows within an optimal pH range of 2.5 - 5.8 During oil recovery operations, iron oxidizing bacteria can diminish the permeability of rock-formations, and their elimination or control from injection water should be mandatory.
Desulfovibrium (non-sporulated)	Strict anaerobes growing between 25 - 44 degrees Celsius and within a pH range of 5.5 - 9.0 (optimum pH = 7.2); Approximate dimensions: 0.5 - 1.0 μm diameter and 3.0 - 5.0 μm long. Some species as <i>D. salexigens</i> require a concentration of 2.5% sodium chloride in the medium.
Desulfotomaculum (sporulated)	Strict anaerobes, and can exist as single cells or short chains. One of the species, <i>Desulfotomaculum nigrifican</i> , is thermophilic with an optimal temperature for growth of 55 degrees Celsius. The upper temperature range for growth is 65 - 70 degrees Celsius, they can be adapted to grow at 30 - 37 degrees Celsius. The existence for these thermophilic strains is important to the injection waters used for secondary oil recovery, where planktonic and sessile SRB are frequently found at temperatures of 70 degrees Celsius and higher. These microorganisms can cause serious problems of biofouling and corrosion in the water injection lines.

The pH range that is optimal for the different bacteria listed in Table 3, varies between a value of 0.5 to 9. The temperature range also varies from a low of 25° C (77° F) to a high of 70° C (158° F). All the bacteria represented in Table 3 can be found in the marine environment, and can be responsible for the souring of oil wells, or the pitting of steel.

The corrosion of pipelines therefore is dependent upon what type of bacteria is present in the system. According to a study performed on the producing wells of 24 oil fields it was concluded that as the temperature and the salinity of a well increases, the bacterial count in the well decreases. In Figure 7 a plot of bacterial count versus the temperature of each well from the study can be seen. [39]

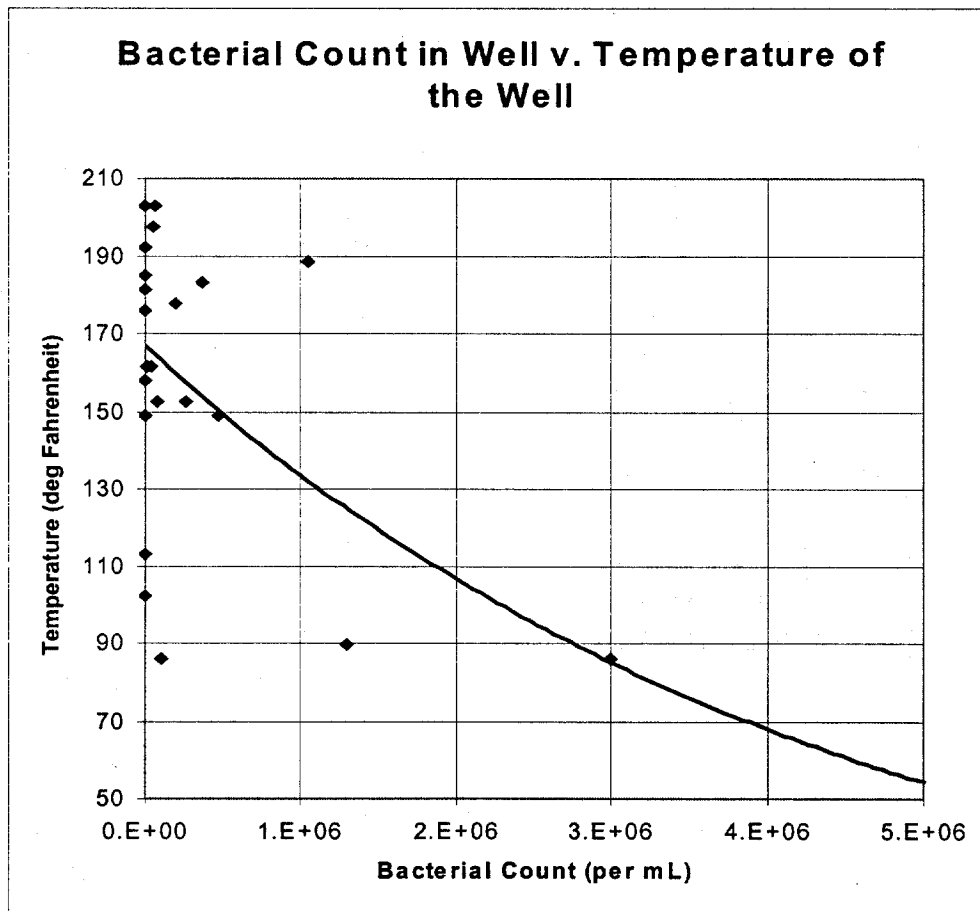


Figure 7: Plot of bacterial count versus well temperature. [39]

The conclusion from the study was that it is more likely for a low temperature well to be sour, due to the fact that it provides a more suitable environment for bacterial growth. There are two hypotheses as to how a well can become sour. The first hypothesis states that as water is pumped into the oil wells during secondary recovery techniques, the indigenous bacteria present in the well are provided with nutrients, which in turn stimulates them to grow. The second hypothesis states that since ocean water contains many types of bacteria, these bacteria when introduced into the oil well, use the nutrients in the well and flourish.

Oil wells often contain connate water that was trapped during the geological formation of the wells, and many times the water supports indigenous bacteria. When the connate water in oil wells are sampled, new species of bacteria are always found, especially in the lower temperature oil wells. This implies that life in the wells is able to flourish, therefore when water is pumped in from the ocean, the sulfate reducing bacteria in the water are able to flourish unimpeded. The question however is which bacteria are more likely to flourish?

Returning to Table 3, it can be seen that certain bacterial types have an optimum temperature and pH range where they are able to grow and flourish at an optimum rate. Most however can evolve and assimilate to their new environment. In Table 4, a list of temperature ranges corresponding to possible localized pH ranges at the surface of the metal can be seen. At the lower temperatures, the possible pH range has lower values, while at the higher temperatures, the pH ranges are near neutral. The explanation for lower temperature ranges having lower possible pH ranges is that sulfate reducing bacteria are more likely to survive at lower temperature. Therefore the more species that survive, the more likely it is that hydrogen sulfide will be produced, and the possible pH therefore will be lower.

TEMPERATURE RANGE OF WELL (°C)	TEMPERATURE RANGE OF WELL (°F)	POSSIBLE pH RANGE
30 – 50	86 – 122	0.5 – 5.0+
50 – 70	122 – 158	2.0 – 6.0+
70 – 90	158 – 194	4.0 – 7.0+
90 – 110	194 – 230	5.0 – 8.0
110 – 140	230 – 284	7.0 – 9.0

Table 4: Possible localized pH ranges on the surface of the metal for various well temperatures.

Calibration of the Corrosion Loss Equation

It is important to note however that for localized pH values to be on the order of 1 and 2, there has to be a biofilm present on the surface of the metal, under which sulfate reducing bacteria are active. Due to the effect of shear stress at the wall of the pipe this might not be possible along certain sections of the pipe, therefore pH ranges at these pipe sections would have to be adjusted.

C. Effect of pH on P and N

From the previous section it was ascertained how sulfate reducing bacteria might affect the value of pH at the liquid metal interface, but the question still remains as to how can the effect of pH be manifested in the values of P and N in the corrosion loss equation.

According to various sources, as the pH of a solution decreases, the corrosion rate tends to increase exponentially. A plot of the effect of pH on the corrosion rate for zinc can be seen in Figure 8.

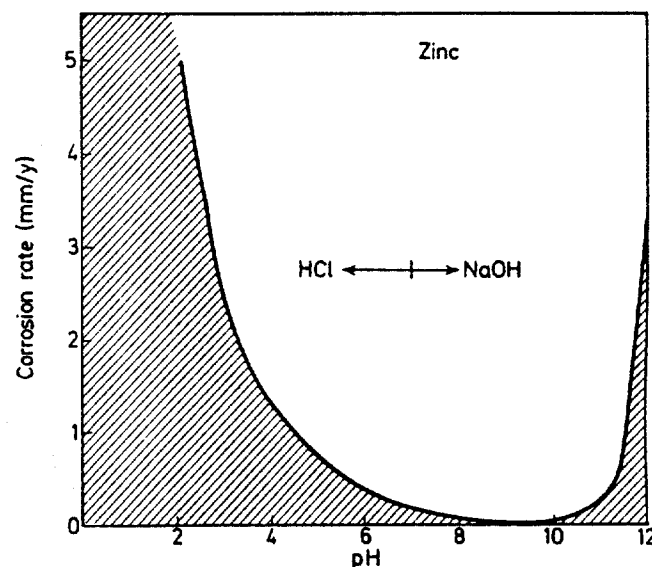


Figure 8: Effect of pH on metals relying on passive films for protection. [8]

The above depiction of the effect of pH on the corrosion rate was used as the basis for developing a rule as to how P and N are affected with decreasing pH. Since P affects the corrosion process directly the following relationship was developed: Corrosion Loss is directly proportional to P. The rule for N is the opposite, where with increasing pH, N decreases.

The key to developing a rule for exactly how pH and P and N are linked together, is to first set a limit on the corrosion loss possible during the first year that the pipe is in service. The limit set on the corrosion loss was 1.3 inches in one year. This value for the corrosion loss was then assigned as the worst corrosion loss possible after one year, for the steel with the highest value of P, mild steel (P = 14). Next the value of P needed to have a corrosion loss of 1.3 inches after one year was determined. The corresponding value of P is 1619.

Since the rule between pH and corrosion rate is exponential, the question becomes, what power does P have to be raised to, to obtain a value of 1619. The answer is 2.8. 2.8 therefore becomes the upper limit for the exponent and now the value of the lower limit must be found. According to Figure 8, the corrosion rate attains its lowest value around a pH of 9, therefore it was decided that at this pH the values of P and N would not change from their original values corresponding to atmospheric corrosion. Equations 3 and 4 illustrate the relationship between pH and the exponent to which P and N are raised.

$$\text{Exponent}_P = \frac{2.80}{pH^n}$$

(Eq. 3)

$$\text{Exponent}_N = \left[\frac{2.80}{pH^n} \right]^{-1}$$

(Eq. 4)

In Equations 3 and 4, n is equal to 0.47, and is the fitting parameter that controls what value the exponent takes at a pH of 9. For n = 0.47, the value of the exponent for P and N at a pH of 9 has the value of 1. Figure 9 shows a graphical representation of the relationship between pH and P and N.

Knowing the effect of pH on P and N, the next task is to determine how the flow regime affects P and N. If the flow in a pipe is turbulent, then there is low probability of a biofilm attaching to the sides of the pipe. Therefore the pH would not be as low as if there were sulfate reducing bacteria growing on the side of the pipe. On the other hand as the flow becomes less and less turbulent, the biofilm has a larger probability of being able to attach itself to the sides of the pipe.

Calibration of the Corrosion Loss Equation

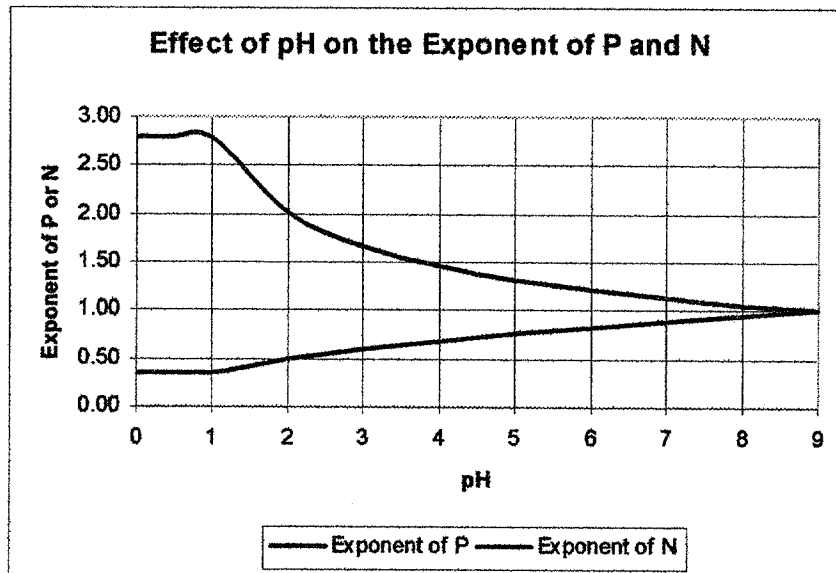


Figure 9: Illustration of the effect of pH on the power to which P or N is raised.

D. Effect of Flow Regime on the Value of P and N

Flow in a multiphase carrying pipe can be difficult to classify, due to several reasons. One reason is that there are at least three major types of fluids present in the pipeline. A multiphase pipeline may carry a certain percentage of oil, gas and water, each of which has a different viscosity, density, and therefore tends to move with a different velocity in the pipe. The rate of the corrosion in the pipeline is directly related however to the velocity of the media within the pipeline.

The corrosion processes in oil and gas production pipelines involve the interaction between metal wall and the flowing fluids. Relative motion between fluid and the metal surface will in general affect the rate of the corrosion. Three theories have been proposed as to how flow affects corrosion. The three ways in which flow can affect corrosion rate are, through convective mass transfer, phase transport, and erosion. For convective mass transfer controlled corrosion, the corrosion rate is affected by either the convective transport of corrosive material to the metal surface or the rate of dissolved corrosion products away from the surface. The phase transport corrosion depends on the wetting of the metal surface by the phase containing corrosive material. The phase distribution is strongly affected by the multiphase flow. Erosion corrosion occurs

when high velocity, high turbulence fluid flow and/or flow of abrasive material prevents the formation of a protective film, allowing fresh material to be continuously exposed to the corrosive environment. The multiphase flow conditions in oil and gas pipelines are also important factors influencing the corrosion and the inhibitor effectiveness. A strong relationship has been found between field measurement of corrosion rate and flow regime.[42]

Figure 10 illustrates the typical flow patterns observed in oil/water/gas flow. At low liquid and gas flow rates, the three phases flow in a smooth stratified pattern. As the gas flow rate is increased, the interface between the oil and gas becomes wavy. If the liquid flows are increased, plug flow is reached.[17]

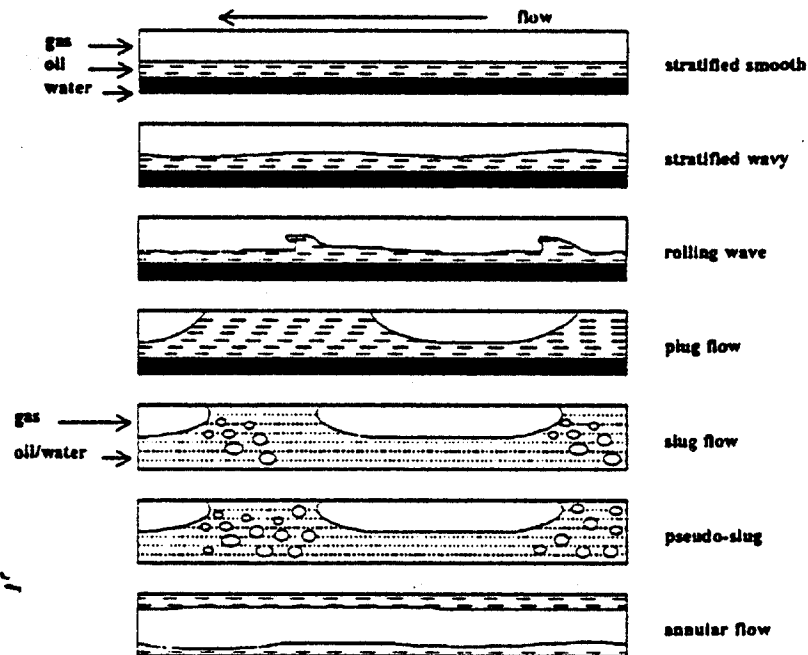


Figure 10: Flow patterns observed in a multiphase pipeline.[17]

In three-phase plug flow, the oil/water interface remains stratified while intermittent gas pockets remove the oil from the top of the pipe. If the gas flow rate is increased from plug flow, slug flow regime is reached. Characteristics of this slug flow include mixing of the oil and water layers, gas pockets of increased length, and gas bubble entrainment in the front of the slug, commonly referred to as the mixing zone. An additional increase in the gas velocity creates a flow pattern termed pseudo slug flow. Pseudo slugs have the same characteristics as slugs, but

the mixing zone extends through the slug length allowing occasional gas blow through to occur. At even higher gas flow rates, annular flow is reached. Annular flow exists when the less dense fluid, the gas, flows in a core along the center of the pipe, while the more dense fluid, the oil/water mixture, flows as an annular ring around the pipe wall.[17]

A study performed at the University of Ohio on multiphase flow in high-pressure horizontal and +5 degree inclined pipelines had the following conclusion:[17]

- The slug frequency increases with increasing liquid flow rate, regardless of liquid composition, inclination and pressure.
- The slug frequency was not variant with pressure.
- Increasing the pressure has no effect upon the stratified/intermittent boundary.
- Increasing the pressure causes pseudo-slug flow to dominate the slug flow regime.
- Increasing the inclination forces the stratified/intermittent boundary to occur at lower liquid flow rates.

Another study performed at the University of Ohio by the same group of researchers, had the following conclusions regarding wall shear stress and flow turbulent intensity near the wall:[42]

- The wall shear stress changes substantially across the front of the slug. The greatest changes occur at high Froude numbers.
- The wall shear stress is always greatest at the bottom of the pipe and decreases towards the top.
- Both the wall shear stress and turbulent intensity increase with an increase in Froude number.
- Adding the oil phase into the flow system increases the wall shear stress but decreases the turbulent intensity.

According to the previous conclusions, several hypotheses can be brought forth. One is that near the well, the velocities in the pipe are large and there is a high probability that there is a lot of turbulence, and also that the shear stress is high. As the flow is examined further down the pipeline, due to head loss in the pipe, the flow velocity decreases due to friction losses. Therefore the second hypothesis states that as the velocity in the pipe decreases the flow regime shifts away from slug flow to plug flow or to stratified flow. The conclusions then are that near the well it is more likely that erosion corrosion along with convective mass transfer corrosion are controlling, but due to the high turbulence bacterial colonies are not able to attach themselves to the pipe walls. As the flow regime changes down the line however, water separates from the oil and the

Calibration of the Corrosion Loss Equation

flow becomes stratified. This enables the bacteria to find suitable conditions to thrive and the water at the bottom of the pipeline is where bacterial colonies tend to be found, which also explains why internal corrosion is predominantly found along the bottom of pipelines.

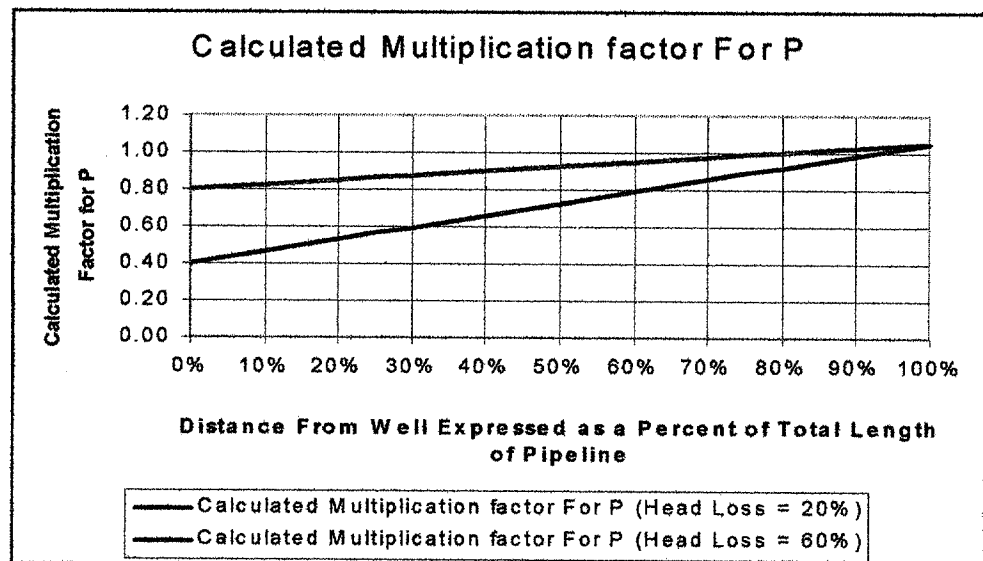
A theoretical equation was derived based on the previous assumptions, which can be seen in Equation 5.

$$MultiplicationFactorForP = \left(105 - \frac{PercentHeadLoss_{OverTotalLength}}{100} \right) \frac{PercentLength_{ofTotalLength}}{100} + \left(\frac{PercentHeadLoss_{OverTotalLength}}{100} + 0.20 \right)$$

(Eq.5)

According to Equation 5, the corrosion rate will depend upon how much head loss there is in the pipeline. The head loss in Equation 5 is taken to be uniform over the length of the pipeline for simplicity. The multiplication factor for P depends upon which point along the line is being examined, and reaches a maximum value of 1.05 at the end of the pipeline. At the front end of the pipeline, the multiplication factor is equal to 0.20 plus the head loss over the total length of the pipeline. The multiplication factor for N on the other hand can be ignored, because N does not have a significant role in the corrosion loss. Figure 11 illustrates the change in the multiplication factor for different values of head loss.

Figure 11:
Illustration of how the multiplication factor changes with total head loss.



To use the diagram in Figure 11, the head loss over the length of the pipeline must be known and the user must decide where the corrosion loss in the pipe is to be calculated: at 50% of the total length or at 75% of the total length. Once the foregoing parameters are known, Equation 5 can be used, or if a set of curves have been developed for various head losses, then the multiplication factor for P can be read directly off of the graph. The value obtained from the graph then can be applied to P, and a correction can be made to the corrosion rate, but this correction factor only applies to a specific section of pipe.

If the pipe is divided into sections for analysis, then the average distance of that section from the well can be used to obtain a value from the graph.

III. Burst Strength of a Corroded Pipe

The burst strength of a pipe will vary according to the amount of section loss that the pipe experienced due to corrosion. The burst strength of an uncorroded pipe can be expressed by Equation 6.

$$P_{allowable} = \frac{\sigma_{yield}t}{r} \quad \text{(Eq. 6)}$$

In Equation 6, t is the thickness of the pipe, r is the outside radius of the pipe, σ_{yield} is the yield stress of the metal, and $P_{allowable}$ is the allowable net pressure that the pipe can operate at before it starts yielding. When corrosion attacks the pipe, many times it is not uniform, especially if sulfate reducing bacteria are present in the system. Figure 12 shows an example of a localized corrosion contour map, where several pits can be seen.

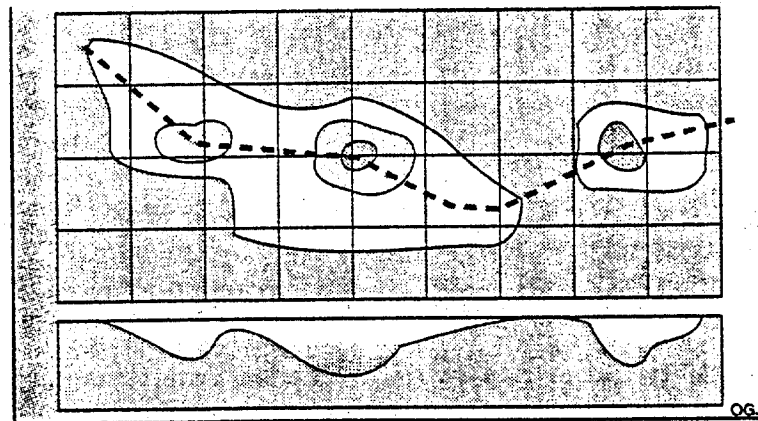


Figure 12: Example of a pit contour map.[28]

In Figure 12, the pits are separated by a certain distance, d , that influences the burst strength of the pipe, and there is also a length associated with the corrosion that also influences the strength of the pipe. To calculate the burst strength of a pipe when only localized corrosion has taken place, Equation 6 has to be modified.

Studies done by ARCO Alaska Inc. have resulted in an equation for the remaining strength of a corroded pipe, and the results of the study are summarized in Equation 7.

$$P = \frac{\left[\frac{2Ft(\sigma_{yield} + 10,000)}{D} \right] \left[1 - \frac{0.85(d + ca)}{t} \right]}{1 - \left(\frac{0.85(d + ca)}{t} \right) \left[3.3 + 0.032 \frac{L^2}{Dt} \right]^{-1}} \quad (\text{Eq. 7})$$

In Equation 7, F is the factor of safety on the pipe, t is the thickness of the pipe, σ_{yield} is the allowable stress in the metal, ca is the corrosion allowance, L is the length of the corrosion, D is the outside diameter of the pipe, d is the depth of corrosion, and P is the allowable pressure. Note however that this equation is only valid for $L^2/Dt > 50$. Another equation is available for situations when $L^2/Dt < 50$, but it is much more complicated and the difference between the two equations is no more than a couple of percent. For this reason the simpler of the two equations has been applied.

Equation 7 is based on the modified ASME/ANSI B31G criterion, which is considered overly conservative. For the modified criterion, the value of the flow stress was modified and equals the specified minimum yield stress plus 10,000 psi, and the cross-sectional area loss was estimated by $0.85 \times L \times d$, which is considered more accurate than the parabolic method, $2/3 \times L \times d$. (See Figure 13)

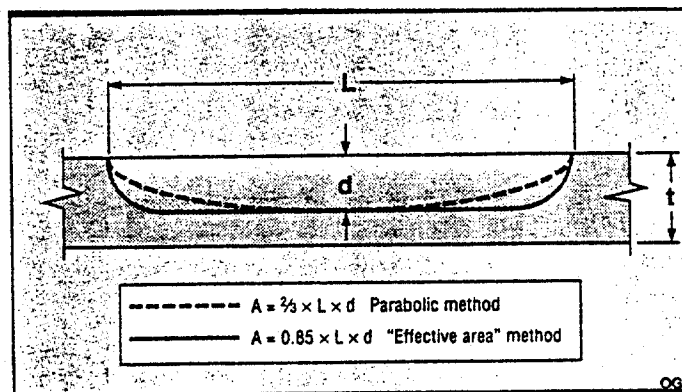


Figure 13: "Effective area" v. parabolic method. [28]

Shell has also done extensive research in the field of burst strength predictions for locally corroded pipes, and obtained results of their own. According to Shell's research, the

maximum pressure that a pipe can withstand before failing can be represented by Equation 8 (Long corrosion model). [43]

$$P^{ref} = \frac{t^*}{R} k^{1+n} \left(\frac{1}{2}\right)^n \sigma_{uts} \quad \text{(Eq. 8)}$$

In Equation 8, P^{ref} is the bursting pressure, t^* is the undeformed corroded wall thickness, R is the undeformed mean radius, k is a yield criterion parameter which is unity for a Tresca yield model and $2/(3)^{1/2}$ for a von Mises yield model, n is the hardening index of the true stress/logarithmic strain curve, and σ_{uts} is the engineering ultimate tensile strength of the material. Note however that this equation is for uniform corrosion, but if the geometry of the corrosion is known in terms of arc length, then the burst pressure can be represented by Equation 9.

$$P = \left(\frac{2}{1 + \phi}\right)^n P^{ref} \quad \text{(Eq. 9)}$$

In Equation 9, ϕ represents the fraction of the pipe wall that has experienced corrosion loss, where if ϕ is equal to $1/4$, it means that out of 360 degrees around the circumference of the pipe, 90 degrees experienced corrosion. If $n = 0.15$ ($n = 2 \times$ circumferential logarithmic strain at burst) and ϕ is close to a value of zero, the extra strength remaining in this pipe compared to the fully corroded pipe is only 10.9 % more. As ϕ becomes larger, the extra strength remaining in the pipe gets smaller, and will be on the order of 7 % for a ϕ equal to $1/4$. Due to the fact however that corrosion can not be accurately measured to this extent, nor predicted, Equation 8 rather than 9 was utilized to derive conclusions about the burst strength of a corroded pipe.

Equations 7 and 8 were applied to several pipe sizes, and the results of the calculations can be seen in Appendix B. The calculations were performed for a 36 inch diameter pipe, and the

Burst Strength of a Corroded Pipe

radius of the pipe was varied from a value of 0.20 inches to 0.45 inches. The yield strength of the steel used is 60,000 psi, and the ultimate strength is taken as 100,000 psi.

A comparison of Equations 7 and 8 can be seen in Figure 14, for a 36 inch diameter pipe having a thickness of 0.45 inches.

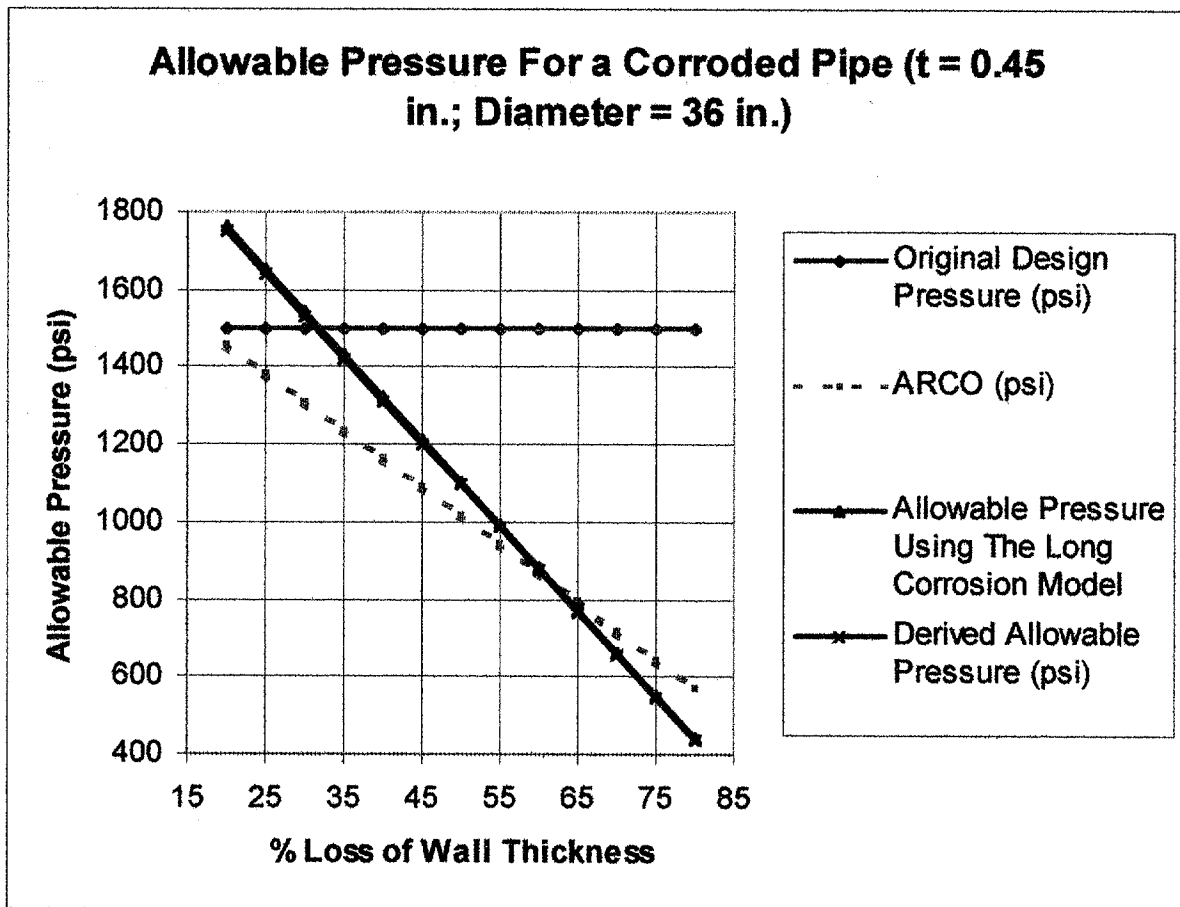


Figure 14: Comparison of various pressure equations.

As can be seen in Figure 14, Shell’s model ($n=0.15, k=1$), obtains allowable pressures well above that of ARCO’s values, up to a value of 60% cross-sectional area loss. As more and more of the area is lost, Shell’s model becomes more conservative than ARCO’s model. It must be kept in mind however that Shell’s model gives values of pressure that are for complete rupture (ultimate), while ARCO’s model uses the yield strength of the material, adjusted by adding 10,000 psi to it. Usually the ultimate tensile strength of a 60,000 psi yield strength steel is 100,000 psi, which clearly explains the difference in the results.

It should also be noted that the operating pressure should never be above that of design. Due to the fact that by operating above the design maximum, a pipeline is more likely to fail, the operating pressure should be reduced when the design pressure is approached in order that some extra utility can be obtained from the pipe before it fails. If there is a factor of safety on the operating pressure, when calculating the reliability, this factor of safety should be included in the bias.

The next task is to obtain a simplified equation for the burst pressure. The simplest approach is to develop an equation similar to Equation 6, which does not deviate from the values of allowable pressure given by Equations 7 and 8. After some trial and error Equation 10 was derived.

$$\Delta P = C \frac{\sigma_{ultimate} t_c}{r} \quad \text{(Eq. 10)}$$

In Equation 10, t_c is the corroded thickness, $\sigma_{ultimate}$ is the ultimate strength of the material and C is a constant whose range is between 0.85 and 0.88. The plot of Equation 10 can be seen in Figure 14, and is designated as the allowable pressure in the pipe. It must be noted however that the pressure defined by Equation 10 is the net pressure on the pipe. Due to hydrostatic forces however, forces can be acting on the outside of the pipe, which could greatly increase the pressure capacity of the pipe. When calculations for allowable pressure are being performed, the effect of external pressure should be taken into consideration in order that the results are not too conservative. The reasons for the development of these equations are so that accurate values of the pressure are obtained, and therefore the pipelines can be operated for longer periods of time. This can result in considerable profit for all operating companies, and also increase the safety of pipelines.

Equation 10 has been designed to fit Shell's solution. It was stated earlier that Shell's solution depends upon strain hardening and utilizes the ultimate tensile strength of the material, therefore it gives values of the ultimate pressure that will burst the pipe. On the other hand ARCO's formula is more conservative for smaller flaw sizes, but for larger flaw sizes, Shell's formula returns more conservative values for the burst pressure. The recommended solution

therefore is to fit Shell's solution, because it utilizes the "true burst strength" of the pipe as opposed to using a quasi stress has a value between 60,000 psi and 100,000 psi. It should also be noted that if the pipe has experienced 20% or less loss in thickness it may be left in service, but if the corrosion loss is 80% of the original thickness or larger, then the pipe section should be replace.

Table 5 shows the percent difference between Equations 7, 8, and 10 for a 36 inch diameter pipe, having an initial thickness of 0.45 inches. Values corresponding to a thickness other than 0.45 can be found in Appendix B.

% LOSS OF THICKNESS	% DIFFERENCE BETWEEN ARCO'S FORMULA AND EQUATION 10	% DIFFERENCE BETWEEN SHELL'S FORMULA AND EQUATION 10
20	-20.37	0.70
25	-18.84	0.70
30	-17.13	0.70
35	-15.21	0.70
40	-13.05	0.70
45	-10.60	0.70
50	-7.80	0.70
55	-4.58	0.70
60	-0.83	0.70
65	3.60	0.70
70	8.90	0.70
75	15.38	0.70
80	23.51	0.70

Table 5: Comparison of ARCO's, and Shell's formula with Equation 10 for various thickness losses. (C = 0.88)

The negative values in Table 5 represent points of Equation 10 that are above that developed by ARCO. The points with a positive percent difference represent points that are more conservative than ARCO's or Shell's formulas.

IV. Reliability of Pipelines

The calculation of the probability of failure of a pipeline requires several characteristics of the system to be known. The probability of failure depends on the type of distribution that the analysis utilizes, how accurate the input is, and whether any biases in the system have been identified and handled appropriately.

For the calculation of the probability of failure, the distribution of failures is assumed to be lognormally distributed. Due to the limited amount of information available this assumption is feasible. If the loading on the system is known, as well as the capacity, the probability of failure can be calculated by Equation 11,

$$P_{failure} = 1 - \Phi(\beta) \quad \text{(Eq. 11)}$$

where β is:

$$\beta = \frac{\ln \left[\frac{P_{Burst50}}{P_{Operating50}} \right]}{\sqrt{\sigma_{\ln B}^2 + \sigma_{\ln O}^2}} \quad \text{(Eq. 12)}$$

In Equation 11, Φ represents the area under the normal distribution curve, and β , the safety index, represents the number of standard deviations from the mean at which the probability of failure is to be calculated. β is calculated using Equation 12, where the median burst and operating pressures are known, and the lognormal standard deviations of the burst and operating pressures are also known.

The lognormal standard deviation of the operating pressure ($\sigma_{\ln S}$) for a typical pipeline system was taken to be 0.20, which corresponds to a coefficient of variation of 20%. The coefficient of variation of the operating pressure is due mostly to pressure surges that may develop during the day to day operation of the pipeline. The bias on the operating pressure is $\frac{1}{2}$, which corresponds to a factor of safety of 2 on the operating

pressure. Pipes are designed for more pressure than they are operated at, therefore the maximum pressure that the pipeline can withstand is usually 1.5 to 2 times the pressure at which the pipeline is operated.

The burst pressure is calculated using Equation 10 in combination with Equation 1. The lognormal standard deviation of the burst pressure is higher than that of the operating pressure due to the fact that there are many sources of variability in the calculation of the depth of corrosion, and in the calculation of the burst pressure. Typical values of $\sigma_{\ln B}$ for an uncorroded pipe are on the order of 0.20 [44], but as there is more and more section loss, the variability in capacity increases due to the fact that there is a high uncertainty associated with the corrosion loss. There is also some uncertainty associated with the calculation of the burst pressure, therefore the lognormal standard deviation of the burst pressure was taken to be $0.20 + (1/100)(\% \text{loss of thickness})$. Using this formulation, the range of values for the lognormal standard deviation is between 0.4 and 1.0, values that are typical for corroded pipes. [44] All losses of thickness under 20% and above 80% are ignored, due to the fact that the accuracy of the burst pressure equation in these regions decreases in accuracy.

For piggable pipelines the determination of acceptable reliability is calculated in the same manner as for unpiggable pipelines, but the lognormal standard deviation is more difficult to determine. One reason why the lognormal standard deviation is difficult to determine is because the spacing of the sensors in a magnetic leakage sensor pig influences the results obtained from the inspection. Other factors also influencing the inspection readings are stresses in the pipe, and the nature of the corrosion, where if the corrosion loss is smooth and gets deeper gradually as opposed to suddenly, the sensors are less likely to detect it. The location of the defect also plays an important role in how accurately the defect is sized, as does the intensity of the magnetic field. [24] For, ultrasonic detection methods, the accuracy of detection is highly dependent on the thickness of the pipe, which is illustrated in Figure 15.

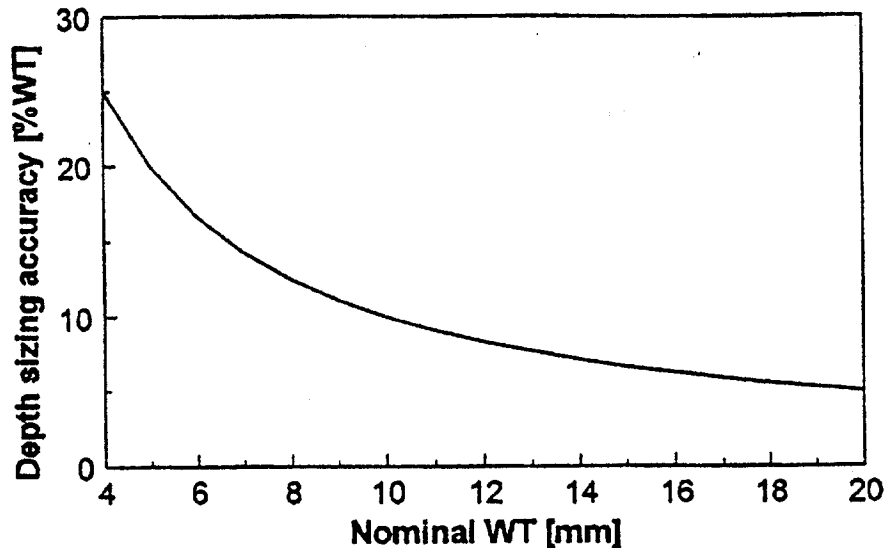


Figure 15: Relative depth sizing error of ultrasonic pigs as a function of wall thickness. [41]

Due to the foregoing reasons, the lognormal standard deviation in the burst pressure for piggable pipelines will be either close to those for unpiggable pipelines or less. For all intensive purposes, the two cases can be treated in the same manner.

Given that all the above parameters can be determined, the calculation of the reliability is performed in the following manner:

- 1. Choose type of material (i.e. Mild Steel, Diameter, Yield Strength, Thickness)**
 - **P and N are determined**
- 2. Determine temperature range of well**
 - **Possible pH is calculated ($pH = 0.034Temp(F) + 0.757$)**
- 3. Adjust P and N according to pH value (Eqs. 3 & 4)**
- 4. Where is the probability of failure to be calculated? (i.e. at 50% total length)**
- 5. What is the total head loss in pipeline due to friction and appurtenances?**
 - **Calculate multiplication factor for P (Eq. 5)**
- 6. Are there any inhibitors in use? How effective are they?**
 - **Adjust P accordingly (i.e. 50% effective = 0.5P)**
- 7. How old is the pipeline (years)**
- 8. Calculate corrosion loss (Eq. 1)**

- **Is the corrosion loss less than 20% \Rightarrow Continue Operation (Make sure operating pressure is at least 1/2 to 2/3 that of design)**
- **Is the corrosion loss greater than 80% \Rightarrow Inspect/Replace Section**

9. Calculate burst pressure (Eq. 10)

10. Determine operating pressure

11. Calculate the safety index, β (Eq. 12)

12. Calculate probability of failure (Eq. 11)

13. Is the probability of failure too high? Too low?

- **Can decrease or increase operating pressure**

- Example Application

An example application was performed using the previous 13 step method for calculating the reliability of a mild steel pipeline, for which the results have been plotted in Figure 16. The type of pipe used for the example was 60,000 psi yield strength pipe, having an outside diameter of 36 inches, and a thickness of 0.75 inches. The temperature of the well was taken as 102° Fahrenheit, which could generate environments with a localized pH value of about 1.9. The distance from the well where the probability of failure was calculated was at 75% of the total length and the head loss in the pipe due to friction and appurtenances was assumed to be 20%. The factor of safety on the operating pressure was taken to be 1.33.

The calculations for the example can be seen in Table 6. The probability of failure calculated for this example is between 4.67 and 76%, which increases as the corrosion loss increases, but the operating pressure is kept the same. The greatest increase in the probability of failure is associated with the operating pressure. If the pressure is reduced with increasing loss of wall thickness, the probability of failure decreases. Figure 17 illustrates the difference in the probability of failure for the pipeline if the factor of safety on the operating pressure is 2 as opposed to 1.33.

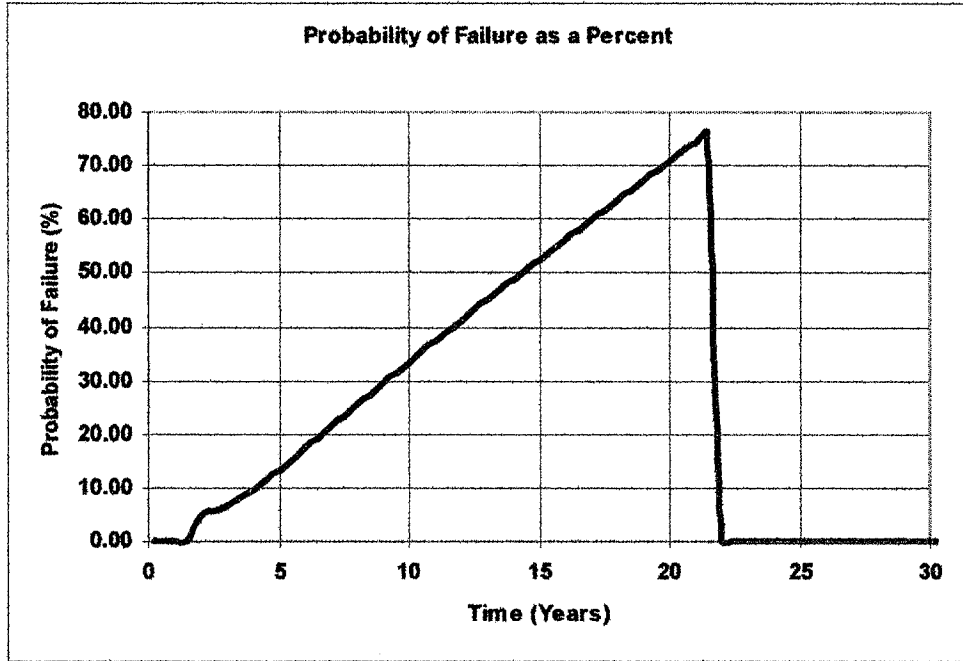


Figure 16: Results of example application.

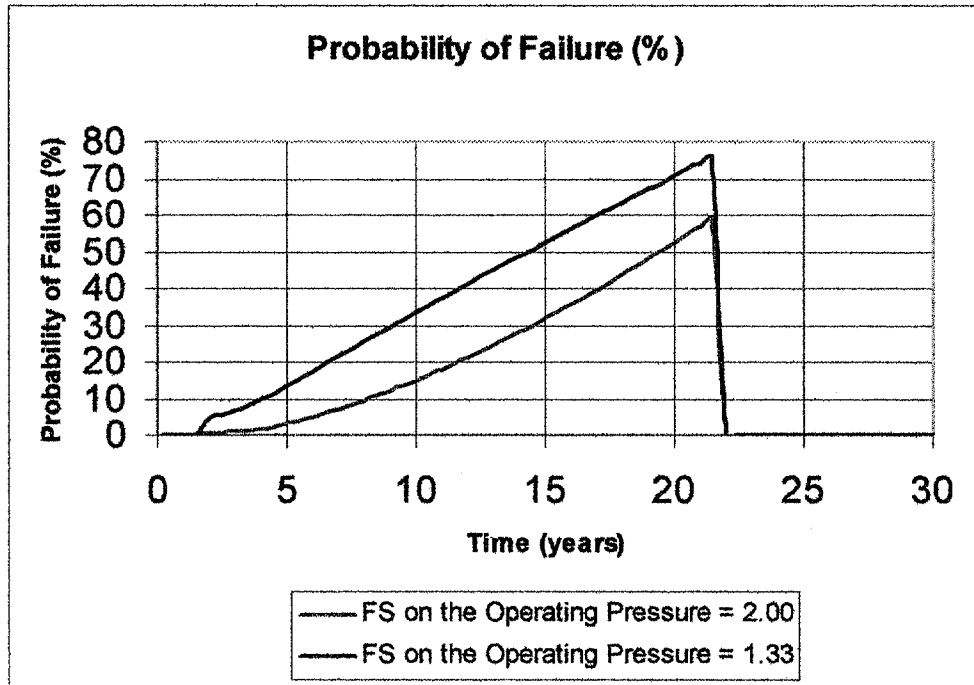
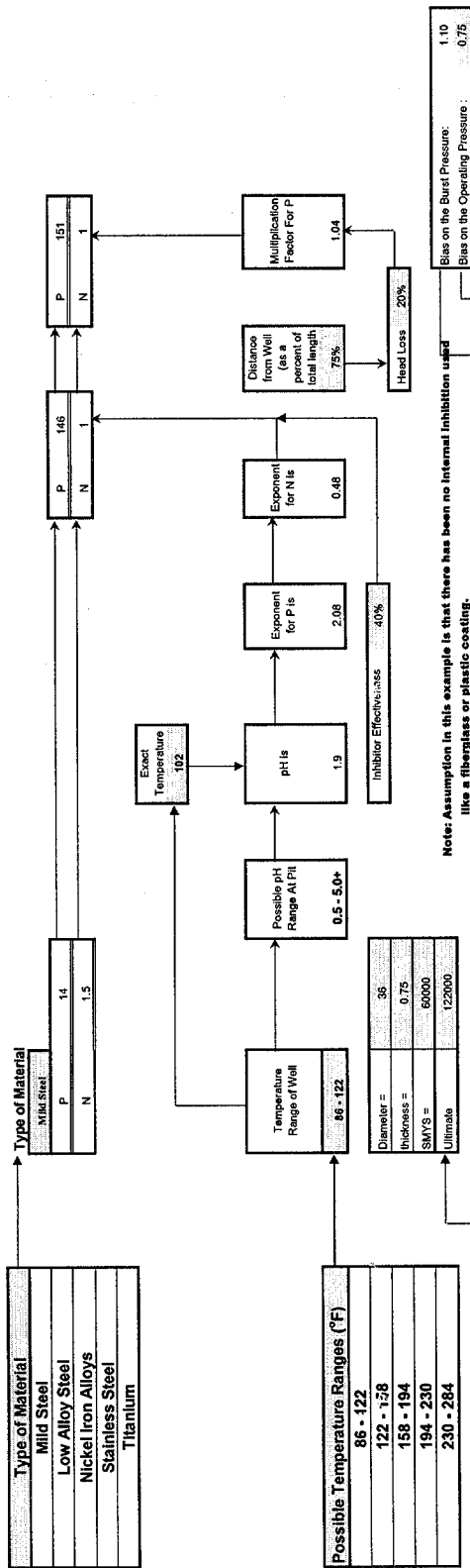


Figure 17: Comparison of varying safety factors on the operating pressure for the example application.

Table 6: Example Problem Illustrating How Reliability Can be Determined by the Developed Formulas



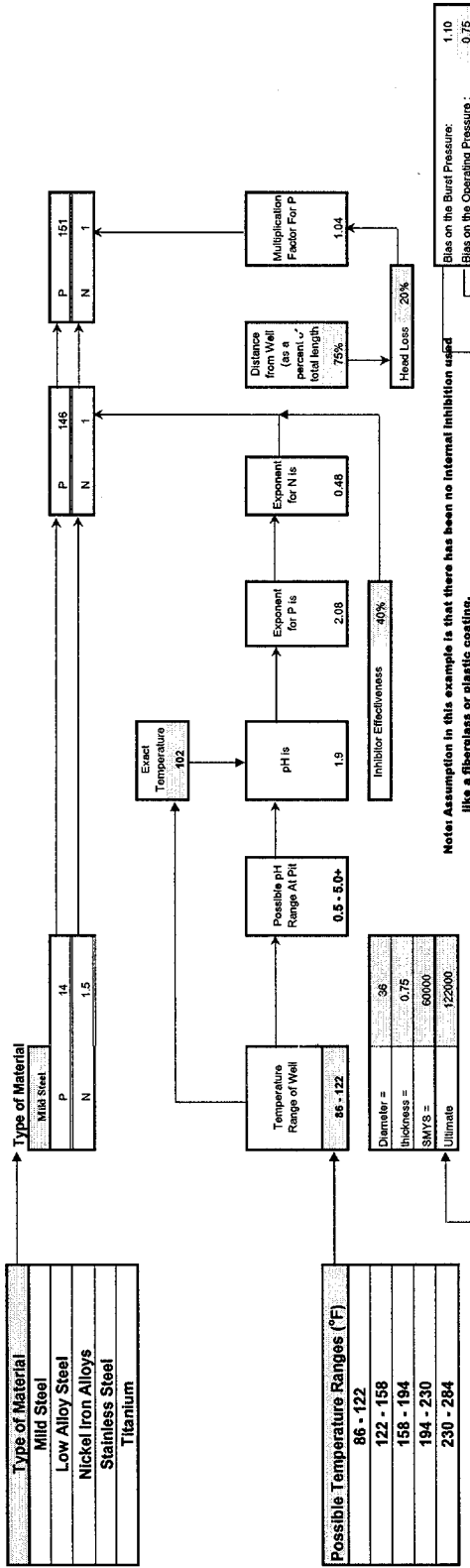
Note: Assumption in this example is that there has been no internal inhibition used like a fiberglass or plastic coating.

Original Design Pressure (psi)	Time Since Pipe was Put in Place (years)	Amount of Corrosion Loss (in.)	% Loss of Wall Thickness	Round Up to Nearest Integer	Allowable Pressure (psi)	Coefficient of Variation of Burst Pressure	σ_{e0}	σ_{n0}	σ_{e0}	MEDIAN Allowable Pressure Solution (psi)	MEDIAN Original Design Pressure (psi)	β	Probability of Failure Percent
2500	0.25	0.05	6.66	Less Than 20% Loss	3578	0.41	0.39	0.2	0.44	3936	1875	1.88	0.047
2500	0.50	0.09	11.65	Less Than 20% Loss	3506	0.42	0.40	0.2	0.45	3856	1875	1.60	0.054
2500	0.75	0.11	14.63	Less Than 20% Loss	3425	0.44	0.42	0.2	0.47	3788	1875	1.50	0.067
2500	1.00	0.12	16.44	Less Than 20% Loss	3338	0.46	0.44	0.2	0.48	3672	1875	1.40	0.081
2500	1.50	0.14	18.50	Less Than 20% Loss	3248	0.48	0.46	0.2	0.50	3572	1875	1.30	0.097
2500	2.00	0.15	20.02	Less Than 20% Loss	3156	0.50	0.47	0.2	0.51	3472	1875	1.20	0.115
2500	2.50	0.16	21.63	Less Than 20% Loss	3065	0.52	0.49	0.2	0.53	3372	1875	1.11	0.133
2500	3.00	0.18	23.43	Less Than 20% Loss	2976	0.54	0.51	0.2	0.54	3273	1875	1.02	0.153
2500	3.50	0.19	25.37	Less Than 20% Loss	2888	0.56	0.52	0.2	0.55	3177	1875	0.94	0.173
2500	4.00	0.21	27.40	Less Than 20% Loss	2803	0.58	0.54	0.2	0.57	3083	1875	0.87	0.193
2500	4.50	0.22	28.45	Less Than 20% Loss	2720	0.60	0.55	0.2	0.59	2892	1875	0.79	0.214
2500	5.00	0.24	31.48	Less Than 20% Loss	2640	0.61	0.56	0.2	0.60	2804	1875	0.73	0.232
2500	5.50	0.25	33.48	Less Than 20% Loss	2561	0.63	0.58	0.2	0.61	2817	1875	0.67	0.253
2500	6.00	0.27	35.43	Less Than 20% Loss	2485	0.65	0.59	0.2	0.63	2733	1875	0.60	0.274
2500	6.50	0.28	37.34	Less Than 20% Loss	2410	0.67	0.61	0.2	0.64	2652	1875	0.54	0.294
2500	7.00	0.29	38.19	Less Than 20% Loss	2338	0.68	0.62	0.2	0.65	2572	1875	0.49	0.313
2500	7.50	0.31	40.99	Less Than 20% Loss	2267	0.70	0.63	0.2	0.66	2493	1875	0.43	0.333
2500	8.00	0.32	42.74	Less Than 20% Loss	2197	0.71	0.64	0.2	0.67	2417	1875	0.39	0.352
2500	8.50	0.33	44.45	Less Than 20% Loss	2129	0.73	0.65	0.2	0.68	2342	1875	0.33	0.372
2500	9.00	0.35	46.11	Less Than 20% Loss	2063	0.74	0.66	0.2	0.69	2269	1875	0.28	0.391
2500	9.50	0.36	47.74	Less Than 20% Loss	1997	0.76	0.68	0.2	0.70	2197	1875	0.23	0.411
2500	10.00	0.37	49.33	Less Than 20% Loss	1933	0.77	0.69	0.2	0.71	2127	1875	0.18	0.430
2500	10.50	0.38	50.88	Less Than 20% Loss									
2500	11.00	0.39	52.40	Less Than 20% Loss									
2500	11.50	0.40	53.89	Less Than 20% Loss									
2500	12.00	0.42	55.35	Less Than 20% Loss									
2500	12.50	0.43	56.78	Less Than 20% Loss									

$$pH = 0.9437 \text{Temp}(F) + 0.7566$$

Actual Value After Adjusted for z Standard Deviations

Table 6: Example Problem Illustrating How Reliability Can be Determined by the Developed Formulas



Note: Assumption in this example is that there has been no internal inhibition used like a fiberglass or plastic coating.

Original Design Pressure (psi)	Time Since Pipe was Put in Place (years)	Amount of Corrosion Loss (in.)	% Loss of Wall Thickness	Round Up to Nearest Integer	Allowable Pressure (psi)	Coefficient of Variation for Burst Pressure	σ _{yo}	σ _{yo}	σ _{he}	MEDIAN Allowable Pressure (psi)	MEDIAN Original Design Pressure (psi)	β	Probability of Failure as a Percent
2500	13.00	0.44	58.19	59	1870	0.79	0.70	0.2	0.72	2057	1875	0.13	0.449
2500	13.50	0.45	59.57	60	1808	0.80	0.70	0.2	0.73	1889	1875	0.08	0.468
2500	14.00	0.46	60.93	61	1748	0.81	0.71	0.2	0.74	1922	1875	0.03	0.487
2500	14.50	0.47	62.27	63	1686	0.83	0.72	0.2	0.75	1957	1875	-0.01	0.505
2500	15.00	0.48	63.59	64	1629	0.84	0.73	0.2	0.76	1992	1875	-0.08	0.524
2500	15.50	0.49	64.88	65	1571	0.85	0.74	0.2	0.76	2028	1875	-0.11	0.543
2500	16.00	0.50	66.16	67	1514	0.87	0.75	0.2	0.78	2065	1875	-0.15	0.561
2500	16.50	0.51	67.42	68	1457	0.88	0.76	0.2	0.78	2103	1875	-0.20	0.579
2500	17.00	0.51	68.66	69	1402	0.89	0.76	0.2	0.79	2142	1875	-0.25	0.598
2500	17.50	0.52	69.89	70	1347	0.90	0.77	0.2	0.80	2182	1875	-0.30	0.616
2500	18.00	0.53	71.09	72	1293	0.92	0.78	0.2	0.81	2223	1875	-0.34	0.634
2500	18.50	0.54	72.29	73	1240	0.93	0.79	0.2	0.81	2264	1875	-0.39	0.652
2500	19.00	0.55	73.46	74	1187	0.94	0.80	0.2	0.82	2306	1875	-0.44	0.670
2500	19.50	0.56	74.63	75	1135	0.95	0.80	0.2	0.83	2349	1875	-0.49	0.688
2500	20.00	0.57	75.78	76	1084	0.96	0.81	0.2	0.83	2392	1875	-0.54	0.707
2500	20.50	0.58	76.91	77	1033	0.97	0.81	0.2	0.84	2436	1875	-0.60	0.725
2500	21.00	0.59	78.03	79	983	0.99	0.83	0.2	0.85	2481	1875	-0.65	0.741
2500	21.50	0.59	79.14	80	933	1.00	0.83	0.2	0.86	2526	1875	-0.70	0.759
2500	22.00	0.60	80.24	Greater Than 80%	Greater Than 80% Loss	—	—	0.2	—	—	1875	—	—
2500	22.50	0.61	81.33	Greater Than 80%	Greater Than 80% Loss	—	—	0.2	—	—	1875	—	—
2500	23.00	0.62	82.40	Greater Than 80%	Greater Than 80% Loss	—	—	0.2	—	—	1875	—	—
2500	23.50	0.63	83.46	Greater Than 80%	Greater Than 80% Loss	—	—	0.2	—	—	1875	—	—
2500	24.00	0.63	84.52	Greater Than 80%	Greater Than 80% Loss	—	—	0.2	—	—	1875	—	—
2500	24.50	0.64	85.56	Greater Than 80%	Greater Than 80% Loss	—	—	0.2	—	—	1875	—	—
2500	25.00	0.65	86.59	Greater Than 80%	Greater Than 80% Loss	—	—	0.2	—	—	1875	—	—
2500	26.00	0.68	88.62	Greater Than 80%	Greater Than 80% Loss	—	—	0.2	—	—	1875	—	—
2500	27.00	0.68	90.62	Greater Than 80%	Greater Than 80% Loss	—	—	0.2	—	—	1875	—	—

$$pH = 0.3437 \text{emp}(F) + 0.7566$$

Conclusion

Determining the reliability of a pipeline is a straightforward process if all the components of the reliability model are known. The developed model, tries to capture the relevant details of the corrosion problem faced by the offshore oil industry, where corrosion due to souring is a major problem.

The souring of wells is caused by bacterial intervention, where sulfate reducing bacteria act to produce hydrogen sulfide and other sulfur compounds that have corrosive characteristics. Wells with lower temperatures, on the order of 100° F, have more potential to sour due to the fact that they offer a good environment for bacteria to grow. Souring of wells is usually accelerated by new recovery techniques, like the pumping of steam or seawater into the well, which either introduces new organisms into the well or provides nutrients for bacteria already present in the connate water of the well.

As the oil, gas and water mixture is recovered, it is transported along the pipeline, where certain flow conditions influence the corrosion process. Due to the fact that a multiphase flow exists in the pipe, under certain conditions high shear stress can develop between the media and the pipe, therefore making it difficult for bacteria or for inhibitors to attach to the side of the pipe. This usually occurs near the well due to the fact that the head loss in the pipe is still minimal, not allowing the oil, gas and water mixture to become fully stratified. As the multiphase mixture travels along the pipe, due to head loss, the velocity decreases, allowing the water to settle out and the mixture stratifies according to density. The water, being the most dense, settles to the bottom and in certain locations stagnates, enabling bacteria to attach to the pipe and to thrive. This is also the reason why most corrosion in pipes is found along the bottom of the pipe.

As bacteria attach to the sides of the pipe, localized pH values may become very low, where in any one bacterial colony there might be several prospering bacterial species. Species that are able to metabolize high amounts of sulfur tend to produce very low pH values, on the order of 2, and tend to cause a lot of damage.

Capturing all the previously mentioned characteristics of a pipeline system, the reliability of the pipeline can be calculated. The model however has to be calibrated for the specific field conditions and the type of metal that the pipeline consists of, in order for it to be more accurate.

It must also be realized that the model was developed through the aid of several references, but actual tests have not been performed to validate the findings. This will have to be done in order for the model to be more reliable. One way to do this is to utilize the databases available through the Minerals Management Service, or to develop new databases that are well organized and maintained.

References

1. Chawla, S. L. and Gupta R. K. Material Selection for Corrosion Control. ASM International. Materials Park, Ohio 1993.
2. Mercer, A. D. Corrosion in Seawater Systems. Ellis Horwood. West Sussex, England 1990.
3. Tousek, J. Theoretical Aspects of the Localized Corrosion of Metals. Trans Tech Publications. Switzerland 1985.
4. Chandler, Kenneth A. Marine and Offshore Corrosion. Butterworth & Co. London, England 1985.
5. Streeter, Victor L. Fluid Mechanics. McGraw Hill. New York, NY 1971.
6. Fink, F. W. and Boyd, W. K. The Corrosion of Metals in Marine Environments. Bayer & Company, Inc. Columbus, Ohio 1970.
7. Videla, Hector A. Manual of Biocorrosion. Lewis Publishers. New York, NY 1996.
8. Shreir, L. L. Corrosion: Volume 1 & Volume 2. Butterworth & Heinemann. Oxford, England 1994.
9. Smith, William F. Foundations of Materials Science and Engineering. McGraw Hill, 2nd edition. New York, NY 1993.
10. Foit, Bruckner A.; Oppermann, Riesch H.; Germerdonk, K. Statistical evaluation of Pig Inspection Data. 1997 OMAE – Vol. II, Safety and Reliability. pp. 243-247
11. Condanni, D. and Barteri, M. Laboratory Testing on Welded Duplex Stainless Steel Line Pipe Internal Corrosion Resistance. 1996 OMAE – Vol. V, Pipeline Technology, ASME 1996. pp. 211-221
12. Dechant, K. E. Effects of High Pressure Testing Technique on Pipelines. 1996 OMAE – Vol. V, Pipeline Technology, ASME 1996. pp. 249-256
13. Hassan, Tariq Al; Robertson, Jacqueline L. M.; Charles, Ellinas; Wickham, Anthony. North Sea Pipeline and Riser Loss of Containment Study – Continuing Improvements. 1996 OMAE – Volume V, Pipeline Technology, ASME 1996. pp. 481-494.
14. Strutt, John E.; Allsopp, Keith; Newman, David; Trille, Christophe. Reliability Prediction of Corroding Pipelines. 1996 OMAE – Volume V, Pipeline Technology, ASME 1996. pp. 495-509.
15. Smith, Liane M.; Celant, Mario. Experience with Corrosion Resistant Pipelines. 1996 OMAE – Volume V, Pipeline Technology, ASME 1996. pp. 549-561.
16. Collberg, Leif; Cramer, Espen H.; Bjornoy, Ola H. Re-qualification of Pipeline Systems. Proceedings of the Sixth (1996) – International Offshore and Polar Engineering Conference (1996) Vol. II. pp. 27-34.
17. Wilkens, Robert; Jepson, Paul W; Studies of Multiphase Flow in High Pressure Horizontal and +5 Degree Inclined Pipes. Proceedings of the Sixth (1996) – International Offshore and Polar Engineering Conference (1996) Vol. II. pp. 139-147.
18. Markin, Andre N. Treating Carbon Dioxide Corrosion in Western Siberian Oilfield Systems. Material Performance, October 1994. pp. 52-55
19. Singleton, Herb. Minimizing Pitting of Tubulars. Material Performance, March 1994. pp. 59-62
20. Donham, James E. Offshore Water Injection System: Problems and Solutions. Material Performance, August 1991. pp. 53-57

21. Petrie, R. R.; Moore Jr., E. M. Determining the Suitability of Existing Pipelines and producing Facilities for Wet Sour Service. Material Performance, June 1989. pp. 59-65
22. Benedict, Risque L. Statistics of a Large Corrosion control Program in Lake Maracaibo. Material Performance, May 1989. pp. 18-24
23. Eagar, R. G.; Leder, J.; Stanley, J. P.; Theis, A. B.; The Use of Glutaraldehyde for Microbiological Control in Waterflood Systems. Material Performance, August 1988. pp. 40-45
24. Hauge, Christian; Atherton, David L; Line Pressure Affects MFL Signals. Oil & Gas Journal, March 18, 1996. pp. 92-99
25. Kim, Hung O.; Model Simplifies Estimate of Bending Strength in Corroded Pipe. Oil & Gas Journal, April 19, 1993 pp. 54-58
26. Roche, Marcel. Systematic Program and Internal Inspection Keys to Corrosion Control. Oil & Gas Journal, April 8, 1991 pp. 72-75
27. Roche, Marcel. Coating Disbondment Leads Causes of External Pipeline Corrosion. Oil & Gas Journal, April 1, 1991 pp. 49-53
28. O'Grady, Thomas J.; Hisey, Daniel T.; Kiefner, John, F.; Pressure Calculation for Corroded Pipe Developed. Oil & Gas Journal, October 19, 1992 pp. 84-89
29. Richardson, David J.; Control of Internal Pipeline Corrosion Based Upon an Evaluation of Risk – A Case for Change. International Pipeline Conference – Volume 1, ASME 1996 pp. 103-110
30. Atherton, D.L.; Czura, W.; Krause, T.W.; R&D Advances in Corrosion and Crack Monitoring for Oil and Gas Pipelines. International Pipeline Conference – Volume 1, ASME 1996 pp. 329-336
31. Peng, C.G.; Park, J.K.; Principal Factors Affecting Microbiologically Influenced corrosion in Carbon Steel. Corrosion – Vol. 50, No. 9 1994 pp. 669-675
32. Little, Brenda; Wagner, Pat. The Impact of Sulfate reducing Bacteria on Welded Copper-Nickel Seawater Piping Systems. Material Performance, August 1988 pp. 57-61
33. Borenstein, Susan Watkins. Microbiologically Influenced Corrosion Failures of Austenitic Stainless Steel Welds. Material Performance, August 1988 pp. 62-66
34. Wagner, Patricia; Little, Brenda. Impact of Alloying on Microbiologically Influenced Corrosion. Material Performance, September 1993 pp. 65-68
35. Walch, Marianne. Introduction: Microbiological Influences on Marine Corrosion. MTS Journal, Vol. 24, No. 3 pp. 3-4
36. Edyvean, R. G. L. The Effect of Microbiologically Generated Hydrogen Sulfide in Marine Corrosion. MTS Journal, Vol. 24, No. 3 pp. 5-9
37. Little, Brenda; Wagner, Patricia; Ray, Richard. Microbiologically Influenced Corrosion in Copper and Nickel Seawater Piping Systems. MTS Journal, Vol. 24, No. 3 pp. 10-17
38. Ford, Tim; Mitchel, Ralph. Metal Embrittlement by Bacterial Hydrogen – An Overview. MTS Journal, Vol. 24, No. 3 pp. 29-35
39. Bernard, F. P.; Connan, Jacques; Indigenous Microorganisms in Connate Water of Many Oil Fields: A New Tool in Exploration and Production Techniques (SPE 24811). Society of Petroleum Engineers 1992 pp. 467-476

40. Stanley, R. K. Magnetic Methods for Wall Thickness Measurement and Flaw Detection in Ferromagnetic Tubing and Plate. Insight, Vol. 38 No. 1, January 1996 pp. 51-55
41. Jansen, H. J. M; Festen, M. M. Intelligent Pigging Developments for Metal Loss and Crack Detection. Insight Vol. 37 No. 6, June 1995 pp. 421-425
42. Sun, Jyi-Yu; Jepson, W. P. Slug Flow Characteristics and Their Effect on Corrosion Rates in Horizontal Oil and Gas Pipelines (SPE 24787). Society of Petroleum Engineers 1992 pp. 215-228
43. Klever, F. J.; Stewart, G; van der Valk, C.A.C. New Developments in Burst Strength Predictions for Locally Corroded Pipelines. Shell International Research, March 1995.
44. Bea, Robert G. Report to PEMEX, IMP and Brown and Root International Inc. November 1997, pp. 19-35

Appendix A

This section contains all data collected for the calibration of Equations 1 and 2. Data was collected for several metal types in several environmental conditions. The data is grouped according to type of metal and amount of exposure time. The location where the data was collected is also included. In the last two columns all fitting parameters valid for the one point provided has been recorded. Corresponding P and N values are grouped in order, where the first P value corresponds to the first N value and so on.

- * For Steel only 10% of oxidation byproduct remains on metal when inspected
- * Low Alloy Steels - Rust is darker in color and finer in grain than formed on ordinary steel
- * When bacteria are present corrosion could be as high as 10 mm/year
- * Atmospheric/Sea water Corrosion Usually is highest around Low Tide Line
- * As one goes deeper and deeper in water the corrosion rate decreases

8 year exposure

Type of Metal	Remarks	Location	Corrosion Loss (mm)	Corrosion Loss (mils)	Corrosion Rate (mm/yr)	Corrosion Rate (mils/yr)	Corresponding P	Corresponding N	
Iron / Wrought Iron									
8 years	Atmosphere	Cristobal, Panama Canal Zone	0.559	22.000	—	—	9.7	—	
8 years	In Pacific Ocean	Off Panama Canal	0.406	16.000	—	—	7.75	—	
8 years	In Pacific Ocean	Oil Panama Canal	—	—	—	—	—	—	
8 years	In Pacific Ocean	Off Panama Canal	—	—	—	—	—	—	
1 year	ingot Iron Exposed for a Year (Salt Content of Air <0.2)	Nigeria	—	—	0.044	1.73	5	5.1	
1	Mild Steel / Carbon Steel / Cast Iron	Rural or Suburban	—	—	0.048	1.890	5	6	
2	1 year	Llanwrtyd Wells	0.200	7.874	0.069	2.717	7,8	6, 4.25	
3	1 year	Teddington	—	—	0.07	2.756	7	6	
4	1 year	Marine	—	—	0.053	2.087	5, 6, 7	7, 4, 1.2	
5	Great Britain	Calshot	—	—	0.079	3.110	10, 7, 4	1.3, 30	
6	1 year	Industrial	—	—	0.095	3.740	11, 10, 9	1, 5.5, 11	
7	1 year	Woolwich	—	—	0.102	4.016	12, 10, 11	1, 7, 5	
8	1 year	Sheffield	0.750	29.528	0.135	5.315	15, 14, 13	1, 5.75, 8.75	
9	1 year	Frodingham	—	—	0.16	6.299	15, 16, 17	1, 7, 5.3	
10	1 year	Derby	—	—	0.17	6.693	19, 18, 17	1, 5, 5.7	
11	1 year	Rural or Suburban	—	—	0.003	0.118	0.2, 0.5	1, 2	
12	1 year	Abisko, North Sweden	—	—	0.005	0.197	0.2, 0.5	10, 0.23	
13	1 year	Delhi	—	—	0.008	0.315	0.3, 0.5	0.25, 10	
14	1 year	Basrah	—	—	0.015	0.591	0.5, 1	0.25, 0.7	
15	1 year	State College, PA, USA	—	—	0.043	1.693	5, 3, 6	6, 0.67, 3	
16	1 year	Berlin-Dahlem	—	—	0.053	2.087	5, 6, 7	7, 4, 1.2	
17	1 year	Marine	—	—	0.015	0.591	0.5, 1	0.25, 0.7	
18	1 year	Apapa, Nigeria	—	—	0.028	1.102	2, 9, 5	1, 1.2	
19	1 year	Sandy Hook, NJ, USA	—	—	0.084	3.307	9.5, 12, 15	1, 3, 1.7	
20	1 year	Marine / Industrial	—	—	0.114	4.488	12.5, 15, 17	1, 3.2, 2.7	
21	1 year	Industrial	—	—	0.108	4.252	12.5, 15, 17	12.5, 15, 17	
22	1 year	Marine, surf beach	—	—	0.615	24.213	—	—	
				Sum	2.072	81.575			
				Mean	0.094	3.708			
				Standard Deviation	0.126	4.965			
				COV	1.339	1.339			
1	0.56	Sea Water	total immersion	—	—	0.143	17.294	—	—
2	0.56	Sea Water	total immersion	—	—	0.143	17.272	—	—
3	0.56	Sea Water	total immersion	—	—	0.148	17.284	—	—
4	0.56	Sea Water	total immersion	—	—	0.143	17.379	—	—
5	0.56	Sea Water	total immersion	—	—	0.140	17.457	—	—
6	0.56	Sea Water	total immersion	—	—	0.140	17.517	—	—
7	0.56	Sea Water	total immersion	—	—	0.136	17.575	—	—
8	0.56	Sea Water	total immersion	—	—	0.143	17.628	—	—
9	0.56	Sea Water	total immersion	—	—	0.158	17.672	—	—

- * For Steel only 10% of oxidation byproduct remains on metal when inspected
- * Low Alloy Steels - Rust is darker in color and finer in grain than formed on ordinary steel
- * When bacteria are present corrosion could be as high as 10 mm/year
- * Atmospheric/Sea water Corrosion Usually is highest around Low Tide Line
- * As one goes deeper and deeper in water the corrosion rate decreases

8 year exposure

Type of Metal	Remarks	Location	Corrosion Loss (mm)	Corrosion Loss (mils)	Corrosion Rate (mm/yr)	Corrosion Rate (mils/yr)	Corresponding P	Corresponding N	
				Sum	1.294	17.559			
				Mean	0.144	17.410			
				Standard Deviation	0.006	0.154			
				COV	0.043	0.009			
1	15 years	Halifax, Nova Scotia	—	—	0.108	4.252	34	1	
2	Mild Steel	Natural Water	Plymouth	—	—	0.065	2.559	20	1
3	5 years	Natural Water	Emsworth	—	—	0.065	2.559	14, 12	1, 3
4	15 years	Natural Water	Plymouth (reservoir)	—	—	0.043	1.683	13	—
5	5 years	Natural Water	La Cadene (granite bed)	—	—	0.068	2.677	14, 12	1.3
6	5 years	Natural Water	Dole (highly calcareous)	—	—	0.010	0.394	2	1.25
	8 years	Natural Water	Rotherham	1.000	39.370	—	—	19.3	—
	15 years	Marine Atmosphere	Colombo, Ceylon	—	—	—	—	—	—
	15 years	Marine Atmosphere	Auckland, New Zealand	2.430	95.669	—	—	31.5	—
	15 years	Marine Atmosphere	Halifax, Nova Scotia	1.640	64.567	—	—	21.2	—
	15 years	Marine Atmosphere	Plymouth, New England	1.090	42.913	—	—	14.2	—
	15 years	Immersion in Sea Water	Colombo, Ceylon	2.550	100.394	—	—	33	—
	15 years	Immersion in Sea Water	Auckland, New Zealand	0.036	1.417	—	—	0.5	—
	15 years	Immersion in Sea Water	Halifax, Nova Scotia	2.150	84.646	—	—	27.7	—
	15 years	Immersion in Sea Water	Plymouth, New England	1.580	62.205	—	—	20.5	—
	15 years	In Sea Water	Colombo, Ceylon	6.500	255.906	—	—	84	—
	15 years	In Sea Water	Auckland, New Zealand	2.590	101.969	—	—	33.5	—
	15 years	In Sea Water	Halifax, Nova Scotia	1.230	48.425	—	—	15.9	—
	15 years	In Sea Water	Plymouth, New England	2.750	108.268	—	—	35.7	—
	15 years	Fresh Water		2.200	86.614	—	—	28.5	—
	8 years	Atmosphere	Cristobal, Panama Canal	0.254	10.000	—	—	4.9	—
	8 years	In Pacific Ocean	Off Panama Canal	1.0795	42.500	—	—	20.6	—
	8 years	In Pacific Ocean	Off Panama Canal	1.5748	62.000	—	—	30	—
	3.3 years	In Sea Water	Harbor Island, NC	—	—	0.053	2.100	13.5, 10, 15	1, 1.33, 0.9
	7.5 years	In Sea Water	Kure Beach, NC	—	—	0.102	4.000	23.7	1
	8 years	In Sea Water	Kure Beach, NC	—	—	0.056	2.200	13	1
	23.6 years	In Sea Water	Santa Barbara, CA	—	—	0.038	1.500	14	1
	16 years	In Sea Water	Panama Canal (Pac. O.)	—	—	0.069	2.700	23	1
	1.5 years	In Sea Water	San Diego (Polluted Sea)	—	—	0.056	2.200	10, 6	1, 12
	5 years	Immersed in Sea Water	Auckland, New Zealand	2.223	87.500	—	—	57	—
	5 years	Immersed in Sea Water	Halifax, Nova Scotia	1.039	40.900	—	—	26.5	—
	5 years	Immersed in Sea Water	Plymouth, New England	1.717	67.600	—	—	43.6	—
	5 years	Immersed in Sea Water	Colombo, Ceylon	3.747	147.500	—	—	95	1
	10 years	Outdoor	Sheffield	0.400	15.748	—	—	8.65	—
	Low Alloy Steels		1st and 2nd years	—	—	0.077	3.031	23.5, 15, 10	1, 1.6, 4
			6th to 15th year	—	—	0.025	0.984	6.6	1
	8 years	Atmosphere	Cristobal, Panama Canal	0.1905	7.5	—	—	3.65	1
	8 years	In Pacific Ocean	Off Panama Canal	—	—	—	—	—	—
	10 years	Outdoor	Sheffield	0.175	6.890	—	—	2.9	—

- For Steel only 10% of oxidation byproduct remains on metal when inspected
- Low Alloy Steels - Rust is darker in color and finer in grain than formed on ordinary steel
- When bacteria are present corrosion could be as high as 10 mm/year
- Atmospheric/Sea water Corrosion Usually is highest around Low Tide Line
- As one goes deeper and deeper in water the corrosion rate decreases

8 year exposure

Type of Metal	Remarks	Location	Corrosion Loss (mm)	Corrosion Loss (mils)	Corrosion Rate (mm/yr)	Corrosion Rate (mils/yr)	Corresponding P	Corresponding N
8 years		Rotherham	0.210	8.268	—	—	4	—
Stainless Steels	0.31	Heavy Industrial site	0.081	3.189	—	—	0.94	—
18 years	1.44	Heavy Industrial site	0.052	2.047	—	—	0.6	—
Atmospheric Exposure Tests	2. —	Heavy Industrial site	0.036	1.398	—	—	0.41	—
18 years	3.45	Heavy Industrial site	0.018	0.689	—	—	0.2	—
18 years	304S15	Rural	0.020	0.787	—	—	0.23	—
18 years	304S15	Semi-industrial	0.021	0.827	—	—	0.24	—
18 years	304S15	Heavy Industrial site	0.081	3.189	—	—	0.94	—
18 years	304S15	Marine	0.085	3.346	—	—	1	—
18 years	316S33	Rural	0.018	0.689	—	—	0.2	—
18 years	316S33	Semi-industrial	0.018	0.709	—	—	0.21	—
18 years	316S33	Heavy Industrial site	0.036	1.398	—	—	0.41	—
18 years	316S33	Manne	0.024	0.945	—	—	0.28	—
Maraging Steels		244m from the sea	—	—	0.005	0.197	1.21	1
8 years		in sea water flowing at 0.6	—	—	0.05	1.969	12, 21	1, 0.4
Nickel Iron Alloys	Fe36Ni	Colombo, Ceylon	0.000	—	—	—	—	—
Marine Atmosphere	Fe36Ni	Auckland, New Zealand	0.000	0.000	—	—	—	—
15 years	Fe36Ni	Halifax, Nova Scotia	0.100	3.937	—	—	1.3	—
15 years	Fe36Ni	Plymouth, New England	0.190	7.480	—	—	2.45	—
Immersion in Sea water	Fe36Ni	Colombo, Ceylon	1.000	39.370	—	—	12.9	—
15 years	Fe36Ni	Auckland, New Zealand	0.240	9.449	—	—	3.1	—
15 years	Fe36Ni	Halifax, Nova Scotia	2.590	101.969	—	—	33.5	—
15 years	Fe36Ni	Plymouth, New England	0.250	9.843	—	—	3.24	—
In Sea Water	Fe36Ni	Colombo, Ceylon	2.500	98.425	—	—	32.4	—
15 years	Fe36Ni	Auckland, New Zealand	1.080	42.520	—	—	14	—
15 years	Fe36Ni	Halifax, Nova Scotia	3.490	137.402	—	—	45	—
15 years	Fe36Ni	Plymouth, New England	1.820	71.654	—	—	23.5	—
Fresh Water (15 yrs)	Fe36Ni		2.000	78.740	—	—	25.8	—
Copper Steel	Atmosphere (8 years)	Cristobal, Panama Canal Zone	0.432	17.000	—	—	5.6	—

Appendix B

This section contains all the calculations for pressure, performed for various thickness of pipe. Equations 7, 8 and 10 are compared and a plot for each is provided. The equations are presented on the next page for convenience. Combinations of various diameter pipe were also examined, besides varying just the thickness of the pipe, and the same conclusions were reached. The differences in the equations are uniform, no matter how the variables are varied, but the derived equation mimics the Shell and ARCO equations more with thicker pipe.

ARCO

$$P = \frac{\left[\frac{2Ft(\sigma_{yield} + 10,000)}{D} \right] \left[1 - \frac{0.85(d + ca)}{t} \right]}{1 - \left(\frac{0.85(d + ca)}{t} \right) \left[3.3 + 0.032 \frac{L^2}{Dt} \right]^{-1}}$$

$$\frac{L^2}{Dt} > 50$$

ca = corrosion allowance
 F = factor of safety
 L = length of corrosion

SHELL

$$P^{ref} = \frac{t^*}{R} k^{1+n} \left(\frac{1}{2} \right)^n \sigma_{uts}$$

t* = undeformed wall thickness of
 corroded patch
 n = hardening index
 k = constant in yield criterion
 φ = corroded section of circumf.

$$P = \left(\frac{2}{1 + \phi} \right)^n P^{ref}$$

$$P_{localisation} = \frac{2^n}{1 + \phi(e^n - 1)} P^{ref}$$

DERIVED

$$\Delta P = C \frac{\sigma_{ultimate} t_c}{r}$$

Table 1: Comparison of Equations for Calculating the Allowable Pressure in a Corroded Pipe

Diameter =	36
Thickness =	0.2
SMYS =	60000

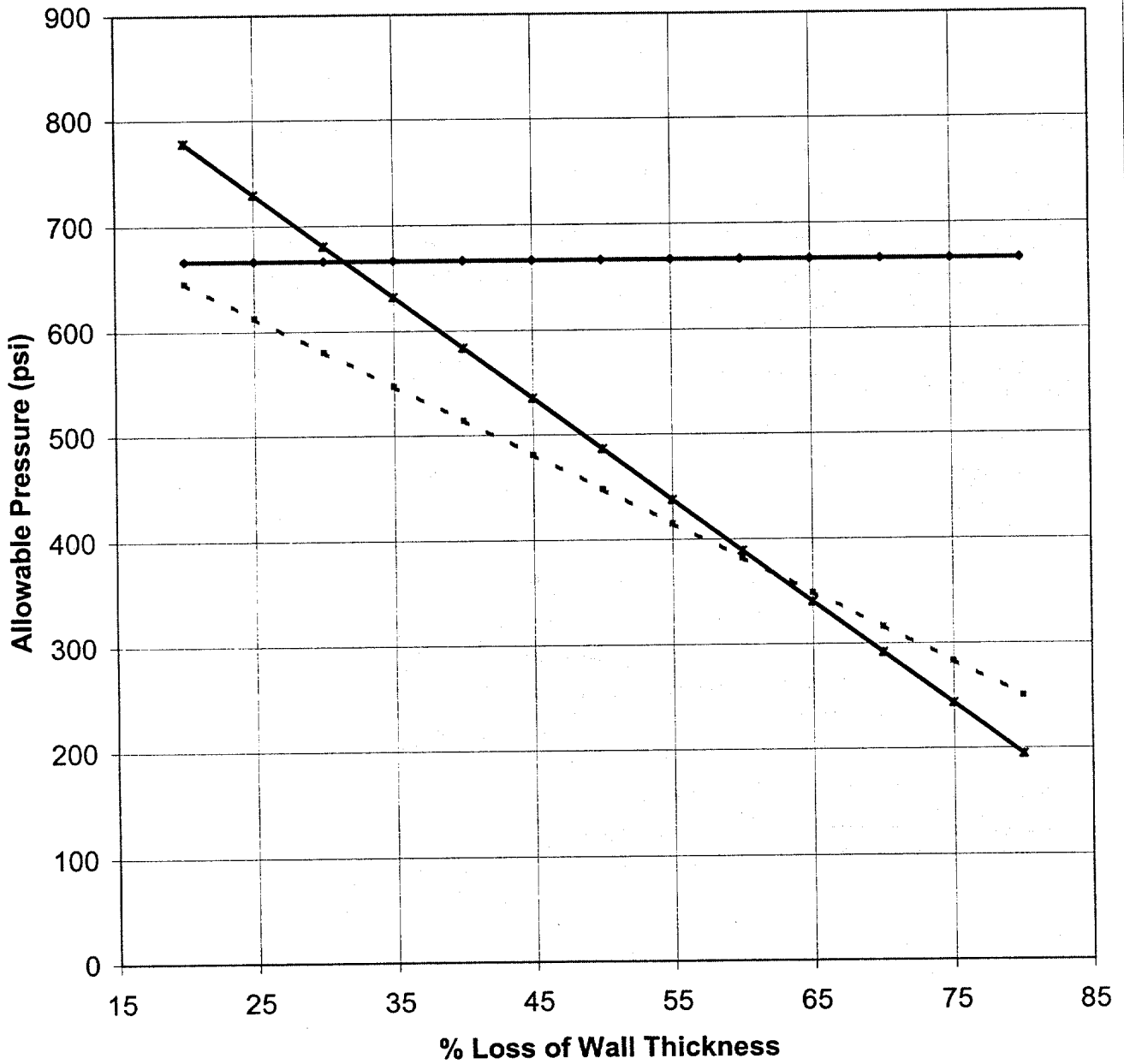
Minimum L^2/dt 18000

n	0.2
R	17.9
k	1
Ult Tens	100,000
t	0.2
ϕ	0.167

Degrees of Corrosion 1.047

Depth of Flaw (in.)	Length of Flaw (in.)	A / A ₀	L ² /dt > 50		Allowable Pressure According to Developments By ARCO (psi)	Allowable Pressure Strength Solution (psi)	Allowable Pressure Using The Long Corrosion Model	With Partly Corroded Circumference	Original Design Pressure (psi)	% Difference Between ARCO's Formula and Strength Solution Multiplication Factor	% Difference Between Shell's Formula and Strength Solution Multiplication Factor	Flaw Size as a % of t
			Allowable Pressure	Strength Solution								
0.04	12	0.170	646	778	646	778	778	667	-20.51	0.00	0.00	20
0.05	12	0.213	613	730	613	730	730	667	-19.05	0.00	0.00	25
0.06	12	0.255	580	681	580	681	681	667	-17.43	0.00	0.00	30
0.07	12	0.298	547	632	547	632	632	667	-15.61	0.00	0.00	35
0.08	12	0.340	514	584	514	584	584	667	-13.56	0.00	0.00	40
0.09	12	0.383	481	535	481	535	535	667	-11.23	0.00	0.00	45
0.10	12	0.425	448	486	448	486	486	667	-8.55	0.00	0.00	50
0.11	12	0.468	415	438	415	438	438	667	-5.45	0.00	0.00	55
0.12	12	0.510	382	389	382	389	389	667	-1.83	0.00	0.00	60
0.13	12	0.553	349	340	349	340	340	667	2.48	0.00	0.00	65
0.14	12	0.595	316	292	316	292	292	667	7.69	0.00	0.00	70
0.15	12	0.638	283	243	283	243	243	667	14.10	0.00	0.00	75
0.16	12	0.680	250	195	250	195	195	667	22.20	0.00	0.00	80

Allowable Pressure For a Corroded Pipe (t = 0.20 in.)



- ◆— Original Design Pressure (psi)
- - - ARCO (psi)
- ▲— Allowable Pressure Using The Long Corrosion Model (psi)
- ×— Derived Allowable Pressure (psi)

Table 2: Comparison of Equations for Calculating the Allowable Pressure in a Corroded Pipe

Diameter =	36
Thickness =	0.25
SMYS =	60000

Minimum L^2/dt 11520

n	0.2
R	17.875
k	1
Ult Tens	100,000
t	0.25
ϕ	0.167
Degrees of Corrosion	
	1.047

Depth of Flaw (in.)	Length of Flaw (in.)	A / A ₀	L ² /dt > 50		Allowable Pressure Using The Long Corrosion Model	With Partly Corroded Circumference	Original Design Pressure (psi)	% Difference Between ARCO's Formula and Strength Solution Multiplication Factor	% Difference Between Shell's Formula and Strength Solution Multiplication Factor	Flaw Size as a % of t
			Allowable Pressure According to Developments By ARCO (psi)	Allowable Pressure Solution (psi)						
0.05	12	0.170	807	973	974	1056	833	-20.49	0.14	20
0.06	12	0.213	766	912	913	990	833	-19.02	0.14	25
0.08	12	0.255	725	851	852	924	833	-17.39	0.14	30
0.09	12	0.298	684	790	791	858	833	-15.56	0.14	35
0.10	12	0.340	643	730	731	792	833	-13.49	0.14	40
0.11	12	0.383	602	669	670	726	833	-11.14	0.14	45
0.13	12	0.425	561	608	609	660	833	-8.44	0.14	50
0.14	12	0.468	519	547	548	594	833	-5.33	0.14	55
0.15	12	0.510	478	486	487	528	833	-1.68	0.14	60
0.16	12	0.553	437	426	426	462	833	2.65	0.14	65
0.18	12	0.595	396	365	365	396	833	7.87	0.14	70
0.19	12	0.638	355	304	304	330	833	14.29	0.14	75
0.20	12	0.680	313	243	244	264	833	22.39	0.14	80

Allowable Pressure For a Corroded Pipe (t = 0.25 in.)

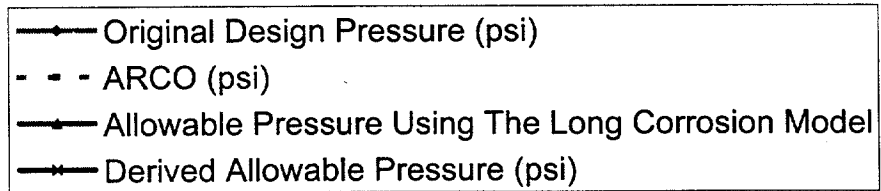
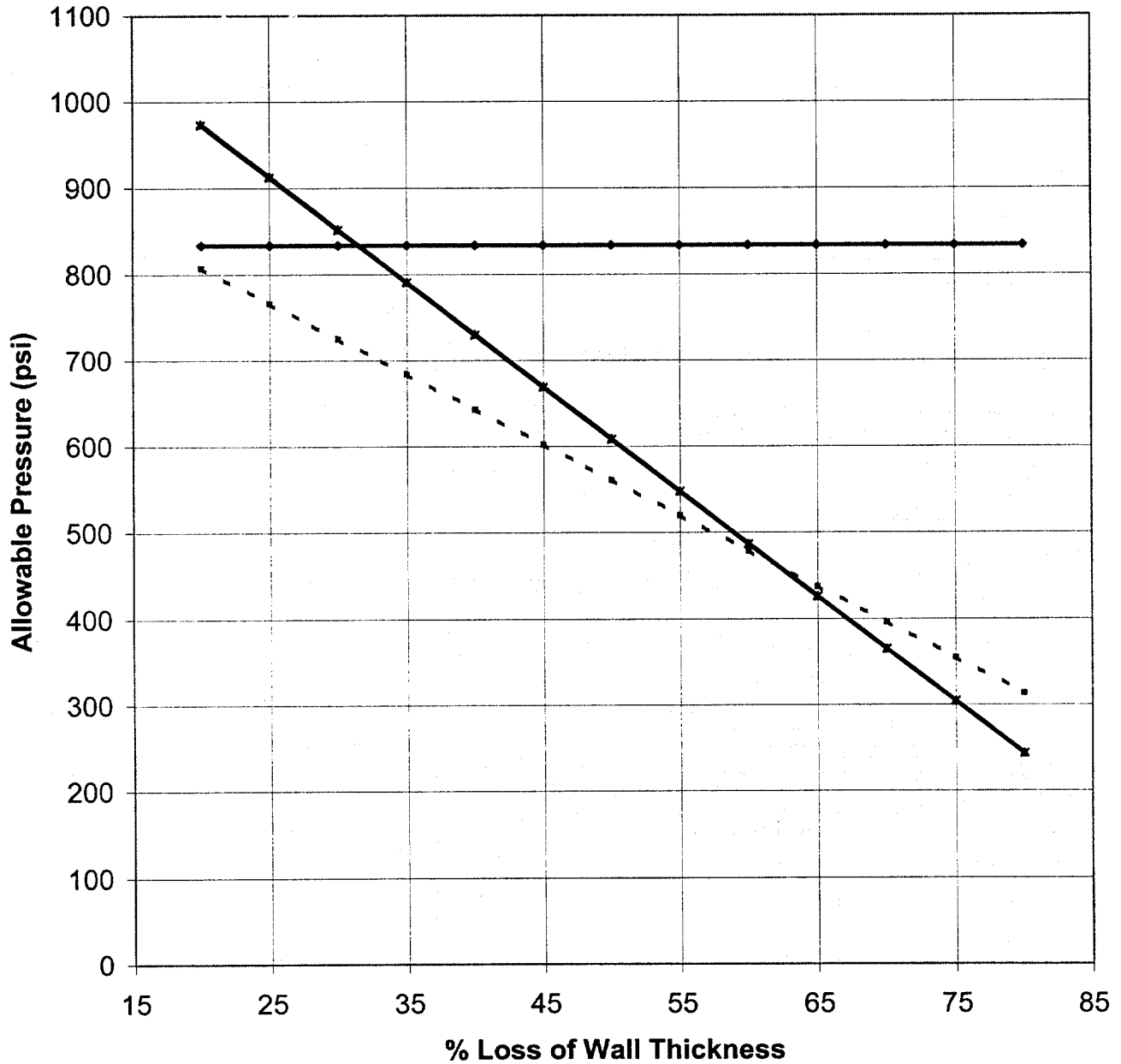


Table 3: Comparison of Equations for Calculating the Allowable Pressure in a Corroded Pipe

Diameter =	36
thickness =	0.3
SMYS =	60000

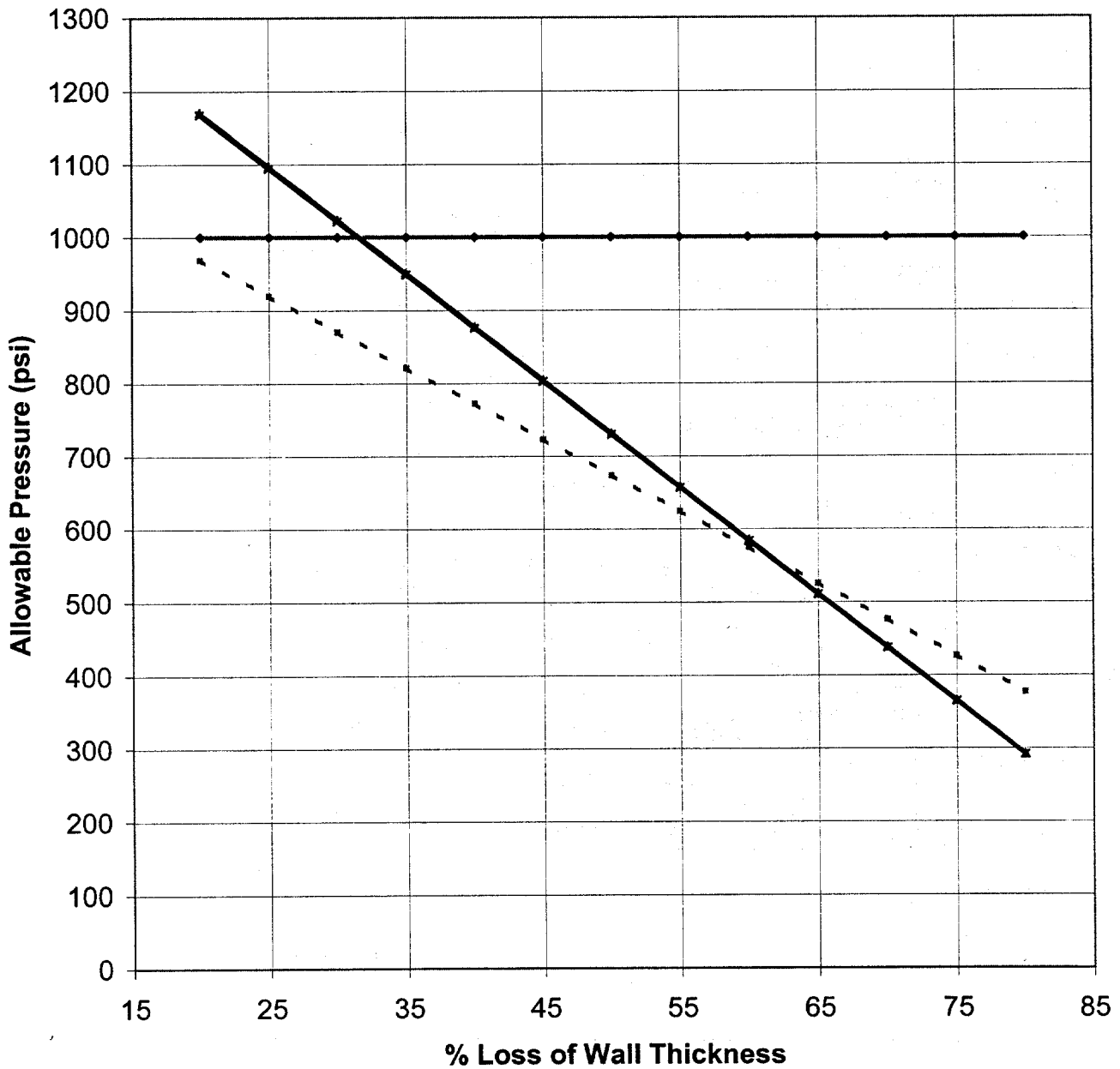
Minimum L^2/dt 8000

n	0.2
R	17.85
k	1
Ult Tens	100,000
t	0.3
ϕ	0.167

Degrees of Corrosion
1.047

Depth of Flaw (in.)	Length of Flaw (in.)	A / A ₀	L ² /dt > 50		Allowable Pressure According to Developments By ARCO (psi)	Allowable Pressure Solution (psi)	Allowable Pressure Using The Long Corrosion Model	With Partly Corroded Circumference	Original Design Pressure (psi)	% Difference Between ARCO's Formula and Strength Solution Multiplication Factor	% Difference Between Shell's Formula and Strength Solution Multiplication Factor	Flaw Size as a % of t
			Allowable Pressure According to Developments By ARCO (psi)	Allowable Pressure Solution (psi)								
0.06	12	0.170	969	1167	1170	1167	1170	1000	-20.46	0.28	0.28	20
0.08	12	0.213	920	1094	1097	1094	1097	1000	-18.99	0.28	0.28	25
0.09	12	0.255	870	1021	1024	1021	1024	1000	-17.34	0.28	0.28	30
0.11	12	0.298	821	948	951	948	951	1000	-15.49	0.28	0.28	35
0.12	12	0.340	772	875	878	875	878	1000	-13.40	0.28	0.28	40
0.14	12	0.383	723	802	805	802	805	1000	-11.03	0.28	0.28	45
0.15	12	0.425	674	730	732	730	732	1000	-8.31	0.28	0.28	50
0.17	12	0.468	624	657	658	657	658	1000	-5.17	0.28	0.28	55
0.18	12	0.510	575	584	585	584	585	1000	-1.50	0.28	0.28	60
0.20	12	0.553	526	511	512	511	512	1000	2.84	0.28	0.28	65
0.21	12	0.595	476	438	439	438	439	1000	8.08	0.28	0.28	70
0.23	12	0.638	427	365	366	365	366	1000	14.52	0.28	0.28	75
0.24	12	0.680	377	292	293	292	293	1000	22.63	0.28	0.28	80

Allowable Pressure For a Corroded Pipe (t = 0.30 in.)



- ◆— Original Design Pressure (psi)
- - - ARCO (psi)
- ▲— Allowable Pressure Using The Long Corrosion Model
- ×— Derived Allowable Pressure (psi)

Table 4: Comparison of Equations for Calculating the Allowable Pressure in a Corroded Pipe

Diameter =	36
thickness =	0.35
SMYS =	60000

Minimum L^2/dt 5878

n	0.2
R	17.825
k	1
Ult Tens	100,000
t	0.35
ϕ	0.167

Degrees of Corrosion 1.047

Depth of Flaw (in.)	Length of Flaw (in.)	A / A ₀	L ² /dt > 50		Allowable Pressure According to Developments By ARCO (psi)	Allowable Pressure Solution (psi)	Allowable Pressure Using The Long Corrosion Model	With Partly Corroded Circumference	Original Design Pressure (psi)	% Difference Between ARCO's Formula and Strength Solution Multiplication Factor	% Difference Between Shell's Formula and Strength Solution Multiplication Factor	Flaw Size as a % of t
			Allowable Pressure According to Developments By ARCO (psi)	Allowable Pressure Solution (psi)								
0.07	12	0.170	1131	1362	1131	1362	1367	1167	-20.44	0.42	20	
0.09	12	0.213	1073	1277	1073	1277	1282	1167	-18.94	0.42	25	
0.11	12	0.255	1016	1192	1016	1192	1197	1167	-17.28	0.42	30	
0.12	12	0.298	959	1106	959	1106	1111	1167	-15.41	0.42	35	
0.14	12	0.340	901	1021	901	1021	1026	1167	-13.30	0.42	40	
0.16	12	0.383	844	936	844	936	940	1167	-10.90	0.42	45	
0.18	12	0.425	787	851	787	851	855	1167	-8.16	0.42	50	
0.19	12	0.468	730	766	730	766	769	1167	-5.00	0.42	55	
0.21	12	0.510	672	681	672	681	684	1167	-1.30	0.42	60	
0.23	12	0.553	615	596	615	596	598	1167	3.07	0.42	65	
0.25	12	0.595	557	511	557	511	513	1167	8.33	0.42	70	
0.26	12	0.638	499	426	499	426	427	1167	14.78	0.42	75	
0.28	12	0.680	442	340	442	340	342	1167	22.89	0.42	80	

Allowable Pressure For a Corroded Pipe (t = 0.35 in.)

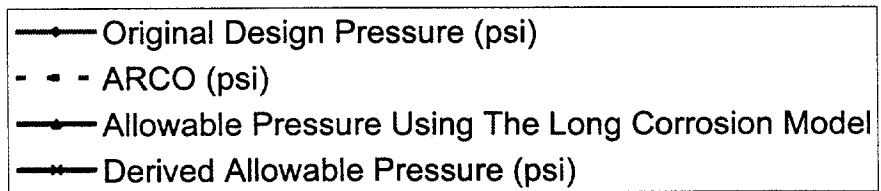
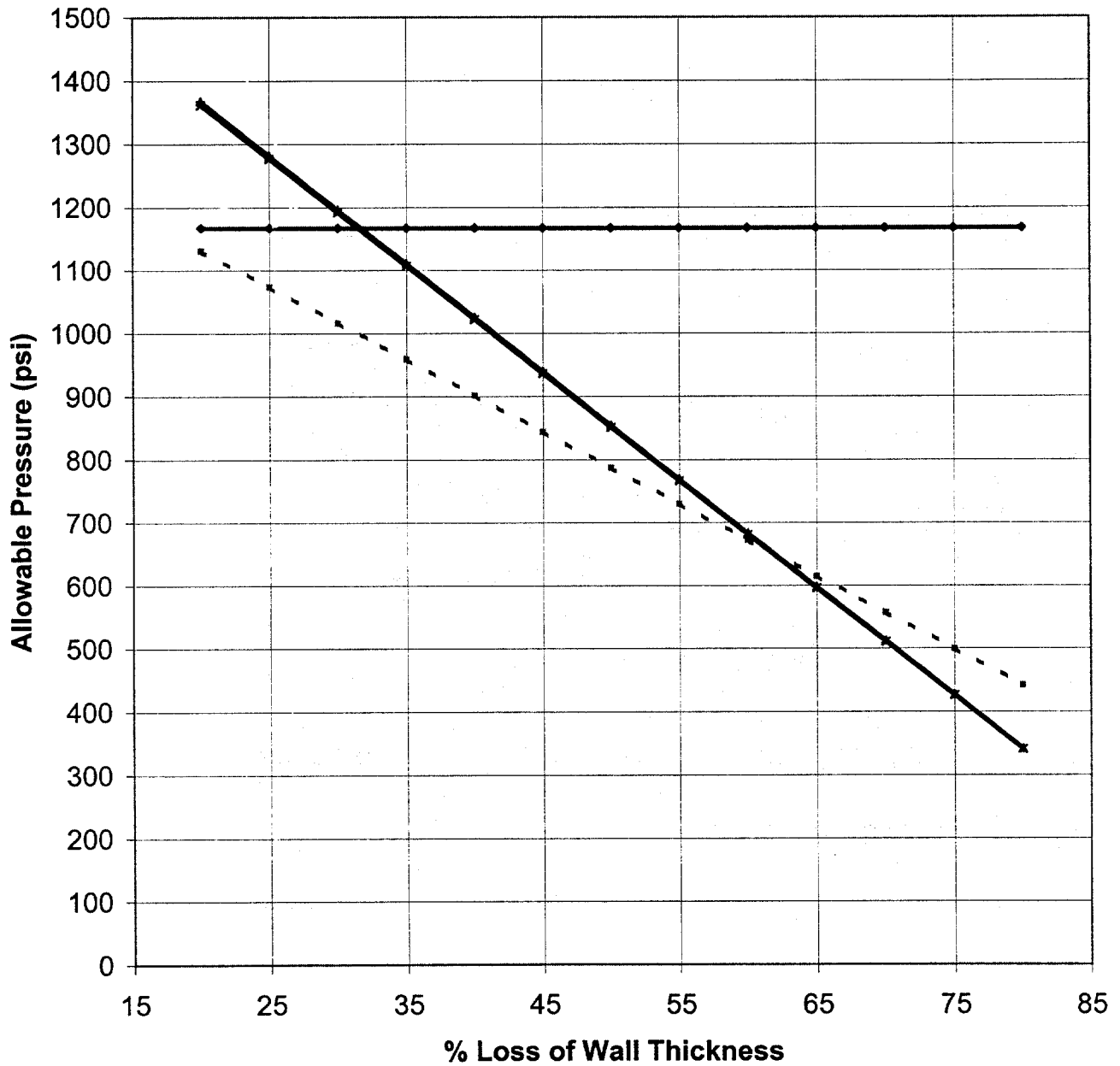


Table 5: Comparison of Equations for Calculating the Allowable Pressure in a Corroded Pipe

Diameter =	36
Thickness =	0.4
SMYS =	60000

Minimum L^2/dt 4500

n	0.2
R	17.8
k	1
Ult Tens	100,000
t	0.4
ϕ	0.167

Degrees of Corrosion 1.047

Depth of Flaw (in.)	Length of Flaw (in.)	A / A ₀	L ² /dt > 50		Allowable Pressure According to Developments By ARCO (psi)	Allowable Pressure Strength Solution (psi)	Allowable Pressure Using The Long Corrosion Model	With Partly Corroded Circumference	Original Design Pressure (psi)	% Difference Between ARCO's Formula and Strength Solution Formula with Multiplication Factor	% Difference Between Shell's Formula and Strength Solution Formula with Multiplication Factor	Flaw Size as a % of t
			Allowable Pressure	Strength Solution								
0.08	12	0.170	1293	1556	1565	1697	1333	-20.40	0.56	20		
0.10	12	0.213	1227	1459	1467	1591	1333	-18.89	0.56	25		
0.12	12	0.255	1162	1362	1369	1485	1333	-17.21	0.56	30		
0.14	12	0.298	1097	1265	1272	1379	1333	-15.31	0.56	35		
0.16	12	0.340	1031	1167	1174	1273	1333	-13.18	0.56	40		
0.18	12	0.383	966	1070	1076	1167	1333	-10.76	0.56	45		
0.20	12	0.425	901	973	978	1061	1333	-7.99	0.56	50		
0.22	12	0.468	835	875	880	954	1333	-4.80	0.56	55		
0.24	12	0.510	770	778	783	848	1333	-1.08	0.56	60		
0.26	12	0.553	704	681	685	742	1333	3.32	0.56	65		
0.28	12	0.595	639	584	587	636	1333	8.60	0.56	70		
0.30	12	0.638	573	486	489	530	1333	15.07	0.56	75		
0.32	12	0.680	507	389	391	424	1333	23.19	0.56	80		

Allowable Pressure For a Corroded Pipe (t = 0.40 in.)

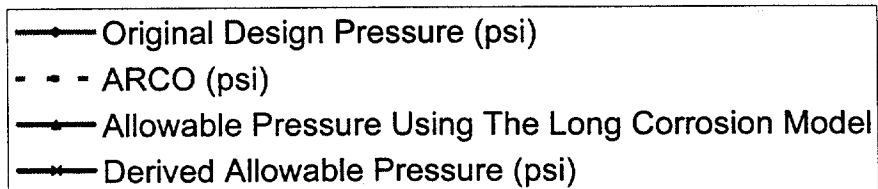
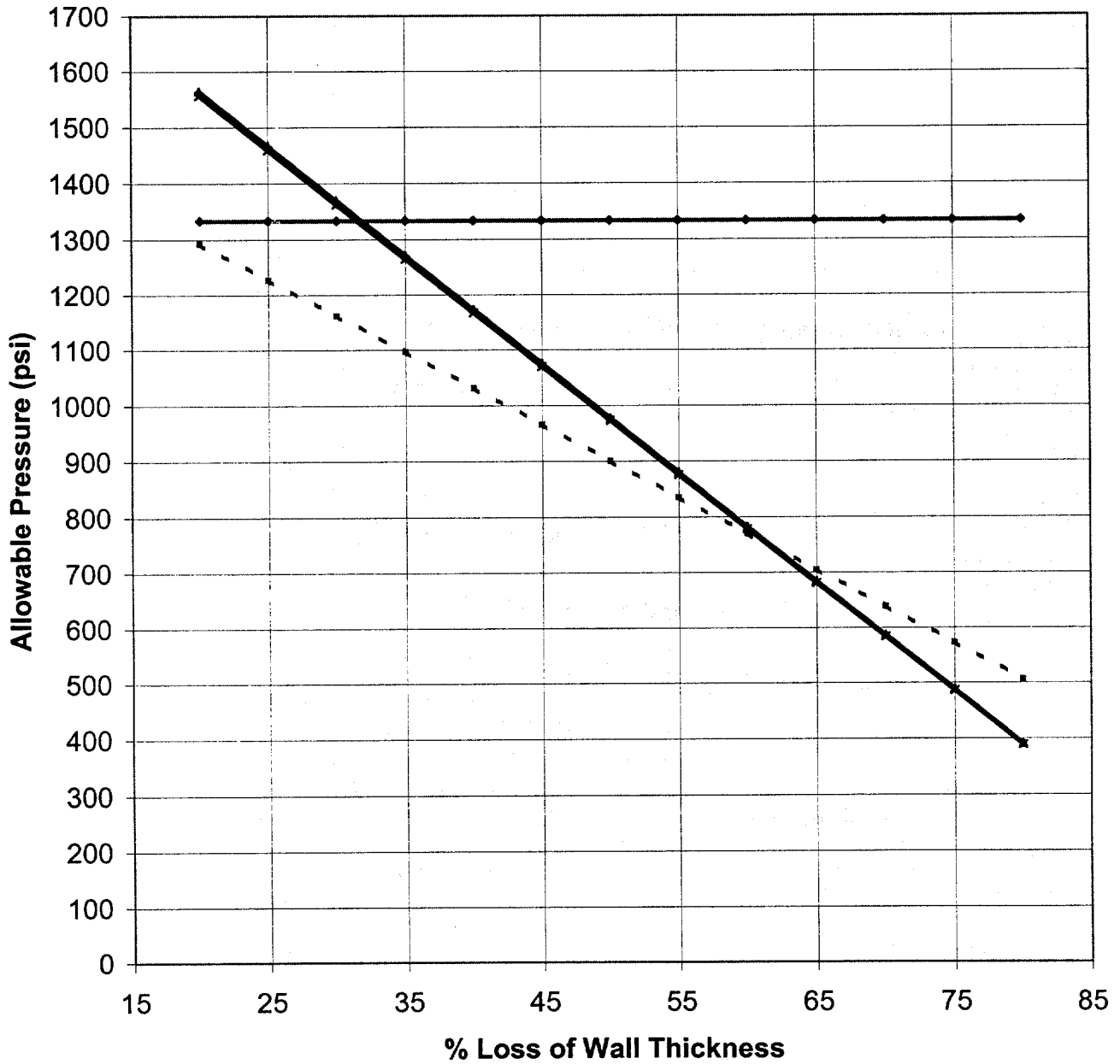


Table 6: Comparison of Equations for Calculating the Allowable Pressure in a Corroded Pipe

Diameter =	36
thickness =	0.45
SMYS =	60000
Minimum L^2/dt	3556

n	0.2
R	17.775
k	1
Ult Tens	100,000
t	0.45
ϕ	0.167

Degrees of Corrosion
1.047

Depth of Flaw (in.)	Length of Flaw (in.)	A / A ₀	L ² /dt > 50		Allowable Pressure According to Developments By ARCO (psi)	Allowable Pressure Solution (psi)	Allowable Pressure Using The Long Corrosion Model	With Partly Corroded Circumference	Original Design Pressure (psi)	% Difference Between ARCO's Formula and Strength Solution Formula with Multiplication Factor	% Difference Between Shell's Strength Solution Formula with Multiplication Factor	Flaw Size as a % of t
			Allowable Pressure	Strength Solution								
0.09	12	0.170	1455	1751	1763	1751	1763	1912	1500	-20.37	0.70	20
0.11	12	0.213	1381	1641	1653	1641	1653	1792	1500	-18.84	0.70	25
0.14	12	0.255	1308	1532	1543	1532	1543	1673	1500	-17.13	0.70	30
0.16	12	0.298	1235	1423	1433	1423	1433	1553	1500	-15.21	0.70	35
0.18	12	0.340	1162	1313	1322	1313	1322	1434	1500	-13.05	0.70	40
0.20	12	0.383	1088	1204	1212	1204	1212	1314	1500	-10.60	0.70	45
0.23	12	0.425	1015	1094	1102	1094	1102	1195	1500	-7.80	0.70	50
0.25	12	0.468	942	985	992	985	992	1075	1500	-4.58	0.70	55
0.27	12	0.510	868	875	882	875	882	956	1500	-0.83	0.70	60
0.29	12	0.553	795	766	771	766	771	836	1500	3.60	0.70	65
0.32	12	0.595	721	657	661	657	661	717	1500	8.90	0.70	70
0.34	12	0.638	647	547	551	547	551	597	1500	15.38	0.70	75
0.36	12	0.680	572	438	441	438	441	478	1500	23.51	0.70	80

Allowable Pressure For a Corroded Pipe (t = 0.45 in.)

